

Statistical mechanics of active Ornstein-Uhlenbeck particles

David Martin^{1,2}, Jérémie O’Byrne,¹ Michael E. Cates,² Étienne Fodor^{1,2,3}, Cesare Nardini,^{4,2}
Julien Tailleur^{1,2}, and Frédéric van Wijland^{1,2}

¹Université de Paris, Laboratoire Matière et Systèmes Complexes (MSC), UMR 7057 CNRS, F-75205 Paris, France

²DAMTP, Centre for Mathematical Sciences, University of Cambridge, Wilberforce Road, Cambridge CB3 0WA, United Kingdom

³Department of Physics and Materials Science, University of Luxembourg, L-1511 Luxembourg

⁴Service de Physique de l’État Condensé, CNRS UMR 3680, CEA-Saclay, 91191 Gif-sur-Yvette, France



(Received 29 August 2020; accepted 23 December 2020; published 11 March 2021)

We study the statistical properties of active Ornstein-Uhlenbeck particles (AOUPs). In this simplest of models, the Gaussian white noise of overdamped Brownian colloids is replaced by a Gaussian colored noise. This suffices to grant this system the hallmark properties of active matter, while still allowing for analytical progress. We study in detail the steady-state distribution of AOUPs in the small persistence time limit and for spatially varying activity. At the collective level, we show AOUPs to experience motility-induced phase separation both in the presence of pairwise forces or due to quorum-sensing interactions. We characterize both the instability mechanism leading to phase separation and the resulting phase coexistence. We probe how, in the stationary state, AOUPs depart from their thermal equilibrium limit by investigating the emergence of ratchet currents and entropy production. In the small persistence time limit, we show how fluctuation-dissipation relations are recovered. Finally, we discuss how the emerging properties of AOUPs can be characterized from the dynamics of their collective modes.

DOI: [10.1103/PhysRevE.103.032607](https://doi.org/10.1103/PhysRevE.103.032607)

I. INTRODUCTION

The hallmark of activity is the lack of connection at the microscopic scale between the injection of energy and its dissipation. While the latter is provided by the environment which, like for an equilibrium colloidal particle, can be an equilibrated liquid, the former arises from the consumption of an independent energy source, whose origin varies from systems to systems. In biology, energy injection typically results from the hydrolysis of adenosine triphosphate (ATP), which drives almost all biological processes such as cell motion [1,2] or intracellular trafficking [3,4]. Synthetic active particles, on the other hand, have been powered using a large range of external sources, whose natures range from chemical [5–7] to electrical [8–11] to mechanical [12–14].

At a theoretical level, the modeling of active systems has been equally diverse, starting either at a coarse-grained, phenomenological level [15–18] or directly at the microscopic scale, using various models of self-propelled particles [19–22]. In the latter case, the standard dynamics of N self-propelled particles typically writes, ignoring inertial effects, as

$$\dot{\mathbf{r}}_i = -\mu \nabla_i \Phi + \mathbf{v}_i, \quad (1)$$

where \mathbf{r}_i describes the position of particle i , \mathbf{v}_i its self-propulsion velocity, μ the particle mobility, and we have included a putative interaction potential $\Phi(\mathbf{r}_1, \dots, \mathbf{r}_N)$. The type of active particles is then specified by the properties of their self-propulsions \mathbf{v}_i . The most studied examples are probably run-and-tumble particles (RTPs) [23] and active

Brownian particles (ABPs) [24], for which \mathbf{v}_i has a constant modulus and reorient either stochastically at a given rate for RTPs or following rotational diffusion for ABPs. These microscopic models and their variants have led to a wealth of surprising behaviors, among which the accumulation at hard boundaries [25,26], the generation of currents by asymmetric obstacles [26–31], the emergence of collective motion [19,32], and motility-induced phase separation (MIPS) [24,33,34].

Whatever the microscopic nonequilibrium origin of self-propulsion, these rich behaviors would be impossible if the \mathbf{v}_i ’s were well described by Gaussian white noises, which would make Eq. (1) an equilibrium dynamics. ABPs and RTPs differ from this simpler case by both the non-Gaussian nature and the persistence of their self-propulsion. Over the past few years, a desire to pinpoint the fundamentals of active matter has led to study simplified models, in which only the non-Gaussian nature [35] or the persistence [36–46] is retained. In this article, we consider the latter case, referred to as active Ornstein-Uhlenbeck particles (AOUPs), which, aside from their theoretical motivations, have also been used to model the motion of passive tracers in an active bath of bacteria [30,47] as well as for the collective dynamics of cells [48,49].

The self-propulsion velocities of AOUPs are given by N independent Ornstein-Uhlenbeck processes:

$$\tau \dot{\mathbf{v}}_i = -\mathbf{v}_i + (2D)^{1/2} \boldsymbol{\eta}_i, \quad (2)$$

where $\{\boldsymbol{\eta}_i\}$ forms a set of zero-mean Gaussian white noises with correlations $\langle \eta_{ia}(t) \eta_{jb}(t') \rangle = \delta_{ij} \delta_{ab} \delta(t - t')$, with Greek indices running over spatial dimensions. It follows that $\{\mathbf{v}_i\}$

forms a set of zero-mean colored Gaussian noises with correlations

$$\langle v_{i\alpha}(t)v_{j\beta}(0) \rangle = \delta_{ij}\delta_{\alpha\beta} \frac{D}{\tau} e^{-|t|/\tau}, \quad (3)$$

where D controls the noise amplitude, and τ quantifies the noise persistence. In the limit of vanishing τ , the self-propulsion velocities \mathbf{v}_i reduce to Gaussian white noises of correlation $\langle v_{i\alpha}(t)v_{j\beta}(s) \rangle = \delta_{ij}\delta_{\alpha\beta}2D\delta(t-s)$. For finite τ , on the contrary, the temporal correlations of the “active noise” \mathbf{v}_i are not matched by a corresponding memory kernel for the instantaneous damping $\gamma \equiv \mu^{-1}$, so that Eq. (1) does not satisfy a FDT of the second kind: it describes a nonthermal process [50]. The correlation time τ hence controls the nonequilibrium properties of the dynamics.

In this article, we study AOUPs both at single-particle and collective levels, and we characterize their static properties as well as their nonequilibrium dynamical features. In Sec. II, we first discuss various limiting cases in which the steady-state distributions of AOUPs can be computed analytically. We discuss in particular the small-persistence-time regime, as well as the impact of nonuniform persistence and activity on the spatial distribution of particles. In Sec. III, we show that AOUPs can undergo MIPS, both in the presence of pairwise purely repulsive forces and due to quorum-sensing interactions if the typical velocity $\sqrt{D/\tau}$ is a sufficiently strongly decreasing function of the local particle density. In Sec. IV, we then turn to characterize dynamically the departure from equilibrium of AOUPs. We first consider the occurrence of particle currents in the presence of ratchet potentials and we then fully characterize the breakdown of time-reversal symmetry. At linear order in τ , we show AOUPs to admit an effective, non-Boltzmann equilibrium regime, which we characterize dynamically in Sec. V by deriving the corresponding generalized fluctuation-dissipation theorem (FDT). Finally, we discuss in Sec. VI the explicit coarse graining of N interacting AOUPs by constructing the dynamics of their collective modes. Note that Secs. II A, IV B, and V A correspond to detailed presentations of results announced in [41] while Sec. II C is a short review on the application of UCNA and Fox theory to AOUPs. All other sections correspond to new material.

II. STEADY-STATE DISTRIBUTION

This section is devoted to the analytical characterization of the stationary distribution of AOUPs. We begin in Sec. II A with the short-persistent-time regime, which has attracted a lot of interest recently [37,38,40–46,51]. We present an expansion to second order in τ and show in Sec. II B how, for a single degree of freedom, it can be extended to higher order. The gap with standard methods developed to characterize the steady state of particles powered by Gaussian colored noises [52–55] is then bridged in Sec. II C. Finally, the steady state of AOUPs with spatially varying activity and persistence is discussed in Sec. II D. Note that Secs. II A–II C are detailed derivations of the results presented in [41], especially for the steady-state distribution (18), and discussions of these results with respect to the existing literature; their content is mostly

technical and they can be omitted during a first reading of the article.

A. Systematic perturbative derivation

Let us start by introducing the particle velocities $\mathbf{p}_i = \dot{\mathbf{r}}_i$ to recast the dynamics of N interacting AOUPS into

$$\tau \dot{\mathbf{p}}_i = -\mathbf{p}_i - (1 + \tau \mathbf{p}_j \cdot \nabla_j) \nabla_i \Phi + (2D)^{1/2} \boldsymbol{\eta}_i, \quad (4)$$

where the mobility has been set to unity. Setting $\tau = 0$ in both sides of Eq. (4) leads to the standard overdamped equilibrium dynamics:

$$\mathbf{p}_i = -\nabla_i \Phi + (2D)^{1/2} \boldsymbol{\eta}_i. \quad (5)$$

Note that setting $\tau = 0$ only in the right-hand side of Eq. (4) also leads to an equilibrium process: the underdamped Kramers equation. More surprisingly, setting $\tau = 0$ in the left-hand side of Eq. (4) also leads to an equilibrium dynamics, albeit with nontrivial mobility and effective potential [37]. This path will be detailed in Sec. II C and we now discuss how a small τ expansion of (4) can instead be *systematically* derived.

Here we follow the treatment introduced in [41] which works with the $\{\mathbf{r}_i, \mathbf{p}_i\}$ variables. In the spirit of [54,56], we first introduce the scaled variables $\tilde{t} \equiv \tau^{-1/2} t$ and $\tilde{\mathbf{p}}_i \equiv \mathbf{p}_i \tau^{1/2}$. As a result, the stationary distribution satisfies $\mathcal{L}P_S(\{\mathbf{r}_i, \tilde{\mathbf{p}}_i\}) = 0$, where the operator \mathcal{L} reads as

$$\begin{aligned} \mathcal{L} = & -\tilde{\mathbf{p}}_i \cdot \nabla_i + \tau^{-1/2} \frac{\partial}{\partial \tilde{p}_{ia}} \left(\tilde{p}_{ia} + \tau \tilde{p}_{j\beta} \frac{\partial^2 \Phi}{\partial r_{i\alpha} \partial r_{j\beta}} \right) \\ & + \frac{\partial}{\partial \tilde{p}_{ia}} \frac{\partial \Phi}{\partial r_{i\alpha}} + D \tau^{-1/2} \frac{\partial^2}{\partial \tilde{p}_{ia}^2}. \end{aligned} \quad (6)$$

Here, and in the following, summations over repeated indices are implicit. (This includes terms like $\tilde{\mathbf{p}}_i^2$ or $\frac{\partial^2}{\partial \tilde{p}_{ia}^2}$.) To compute the stationary distribution, we propose the following ansatz:

$$P_S(\mathbf{r}, \tilde{\mathbf{p}}) \sim e^{-\frac{\Phi}{D} - \frac{\tilde{\mathbf{p}}_i^2}{2D}} \left(1 + \sum_{n=2}^{\infty} \tau^{\frac{n}{2}} A_n(\mathbf{r}, \tilde{\mathbf{p}}) \right), \quad (7)$$

where, for convenience, we define $A_0 \equiv 1$ and $A_1 \equiv 0$, and we introduce the notation $\mathbf{r} = \{\mathbf{r}_i\}$, $\tilde{\mathbf{p}} = \{\tilde{\mathbf{p}}_i\}$, which lightens the notations in the many-particle case. Note that, for normalization purposes, $\int e^{-\frac{\Phi}{D} - \frac{\tilde{\mathbf{p}}_i^2}{2D}} A_n d\tilde{\mathbf{p}} d\mathbf{r}$ has to vanish. We then obtain a set of recursive equations for the A_n equating every order in $\tau^{1/2}$:

$$\left(\tilde{p}_{ia} \frac{\partial}{\partial \tilde{p}_{ia}} - D \frac{\partial^2}{\partial \tilde{p}_{ia}^2} \right) A_n = f_n(\mathbf{r}, \tilde{\mathbf{p}}), \quad (8)$$

where

$$\begin{aligned} f_n(\mathbf{r}, \tilde{\mathbf{p}}) = & -\tilde{p}_{ia} \frac{\partial A_{n-1}}{\partial r_{ia}} + \frac{\partial \Phi}{\partial r_{ia}} \frac{\partial A_{n-1}}{\partial \tilde{p}_{ia}} + \frac{\partial^2 \Phi}{\partial r_{ia}^2} A_{n-2} \\ & - \frac{\tilde{p}_{ia} \tilde{p}_{j\beta}}{D} \frac{\partial \Phi}{\partial r_{ia} \partial r_{j\beta}} A_{n-2} + \tilde{p}_{ia} \frac{\partial^2 \Phi}{\partial r_{ia} \partial r_{j\beta}} \frac{\partial A_{n-2}}{\partial \tilde{p}_{j\beta}}. \end{aligned} \quad (9)$$

Inspection of (8) suggests an ansatz for the A_n in the form of degree- n polynomials in the momenta. [If this is assumed for A_k with $k \leq n$, then A_{n+1} is a polynomial of degree

$(n+1)$.] It can be also checked that A_{2n} contains only even terms in the momenta and A_{2n+1} only odd ones. This results from the symmetry of the equation $\mathcal{L}P_S = 0$ under the transformation $\{\tau^{1/2}, \bar{\mathbf{p}}\} \rightarrow -\{\tau^{1/2}, \bar{\mathbf{p}}\}$. We use the following notation:

$$A_n = \bar{p}_{i_1, \alpha_1} \cdots \bar{p}_{i_n, \alpha_n} \frac{a_{i_1, \dots, i_n, \alpha_1, \dots, \alpha_n}^{(n,n)}}{n!} + \bar{p}_{i_1, \alpha_1} \cdots \bar{p}_{i_{n-2}, \alpha_{n-2}} \frac{a_{i_1, \dots, i_{n-2}, \alpha_1, \dots, \alpha_{n-2}}^{(n,n-2)}}{(n-2)!} + \dots, \quad (10)$$

where the $a^{(m,n)}$'s depend on the particles' positions. Note that A_n contains a $\bar{\mathbf{p}}$ -independent term $a^{(n,0)}$ only if n is even. Note also that (10) is a local function of the momenta, which could be restrictive, but still allow for nonlocal dependence on the particle positions, something known to be important for active particles [57,58].

Plugging the expression (10) for A_n in (8), and equating order by order in $\bar{\mathbf{p}}$, yields explicit expressions of all tensors $a^{(n,m)}$ for $0 < m \leq n$. For even n , this leaves $a^{(n,0)}$ unconstrained (whereas $a^{(2k+1,0)} = 0$ by definition) but constrains $a^{(n-2,0)}$. For instance, we get, for $n = 2, 3, 4$,

$$A_2 = -\frac{(\bar{\mathbf{p}}_i \cdot \nabla_i)^2 \Phi}{2D} + a^{(2,0)}(\{\mathbf{r}_i\}), \quad (11)$$

$$A_3 = \frac{(\bar{\mathbf{p}}_i \cdot \nabla_i)^3 \Phi}{6D} + (\bar{\mathbf{p}}_i \cdot \nabla_i) \nabla_j^2 \Phi - \frac{1}{2D} (\bar{\mathbf{p}}_i \cdot \nabla_i) (\nabla_j \Phi)^3 - (\bar{\mathbf{p}}_i \cdot \nabla_i) a^{(2,0)}, \quad (12)$$

$$A_4 = \frac{1}{8D^2} [(\bar{\mathbf{p}}_i \cdot \nabla_i)^2 \Phi] [(\bar{\mathbf{p}}_j \cdot \nabla_j)^2 \Phi] - \frac{(\bar{\mathbf{p}}_i \cdot \nabla_i)^4 \Phi}{24D} - \frac{(\bar{\mathbf{p}}_i \cdot \nabla_i)^2 [a^{(2,0)} - \nabla^2 \Phi]}{2} + \frac{3}{4D} \frac{\partial \Phi}{\partial r_{i\alpha}} \frac{\partial}{\partial r_{j\alpha}} (\bar{\mathbf{p}}_i \cdot \nabla_i)^2 \Phi + \frac{1}{2D} \frac{\partial [(\bar{\mathbf{p}}_j \cdot \nabla_j) \Phi]}{\partial r_{i\alpha}} \frac{\partial [(\bar{\mathbf{p}}_k \cdot \nabla_k) \Phi]}{\partial r_{i\alpha}} + a^{(4,0)}. \quad (13)$$

The lowest order in $\bar{\mathbf{p}}$ of Eq. (8) for A_n of the form (10) also yields

$$\left(D \frac{\partial^2}{\partial r_{i\alpha}^2} - \frac{\partial \Phi}{\partial r_{i\alpha}} \frac{\partial}{\partial r_{i\alpha}} \right) a^{(n-2,0)} = g_n, \quad (14)$$

where g_n are functions of the particle positions which can be computed explicitly. Finding a solution to (14) thus provides a closed expression for the expansion up to order $n-2$.

From the Fredholm alternative theorem, the condition under which (14) admits a solution, and the expansion can be carried out, is that g_n is orthogonal to $e^{-\Phi/D}$ [59]. This is always possible in the small D limit, following [60], but the existence of solution to arbitrary order remains, in the general case, an open problem. Here, we show that it can be carried out explicitly up to order $\tau^{3/2}$. g_4 indeed reads as

$$g_4 = \frac{1}{D} \frac{\partial^2 \Phi}{\partial r_{i\alpha} \partial r_{j\beta}} \frac{\partial \Phi}{\partial r_{i\alpha}} \frac{\partial \Phi}{\partial r_{j\beta}} - \frac{5}{2} \frac{\partial^3 \Phi}{\partial^2 r_{i\alpha} \partial r_{j\beta}} \frac{\partial \Phi}{\partial r_{j\beta}} - \frac{\partial^2 \Phi}{\partial r_{i\alpha} \partial r_{j\beta}} \frac{\partial^2 \Phi}{\partial r_{i\alpha} \partial r_{j\beta}} + \frac{3D}{2} \frac{\partial^4 \Phi}{\partial^2 r_{i\alpha} \partial^2 r_{j\beta}} \quad (15)$$

and (14) is solved, for $n = 2$, by

$$a^{(2,0)} = -\frac{1}{2D} (\nabla_i \Phi)^2 + \frac{3}{2} \nabla_i^2 \Phi. \quad (16)$$

This yields the following expression for the stationary measure of N interacting AOUPs, valid up to order $\tau^{3/2}$,

$$P_S \sim e^{-\frac{\Phi + \bar{\mathbf{p}}_i^2/2}{D}} \left\{ 1 - \frac{\tau}{2D} [(\nabla_i \Phi)^2 + (\bar{\mathbf{p}}_i \cdot \nabla_i)^2 \Phi - 3D \nabla_i^2 \Phi] + \frac{\tau^{3/2}}{6D} (\bar{\mathbf{p}}_i \cdot \nabla_i) [(\bar{\mathbf{p}}_j \cdot \nabla_j)^2 - 3D \nabla_j^2] \Phi + O(\tau^2) \right\}. \quad (17)$$

The velocity distribution obtained by integrating over the particle position is Gaussian to first order in τ , with the same variance as in [61], obtained within the unified colored-noise approximation (UCNA) framework that we discuss in Sec. II C. However, the $\tau^{3/2}$ order shows that the velocity distribution is non-Gaussian to this order.

Integrating over velocities, we obtain the many-body marginal distribution, in position space, $P_S(\{\mathbf{r}_i\})$:

$$P_S(\{\mathbf{r}_i\}) \sim \exp \left[-\frac{\Phi}{D} - \frac{\tau}{2D} (\nabla_i \Phi)^2 + \tau \nabla_i^2 \Phi + O(\tau^2) \right]. \quad (18)$$

We can now use expression (18) to define an effective potential through $\Phi_{\text{eff}} = -D \ln P_S(\{\mathbf{r}_i\})$ which provides an intuitive picture of how self-propulsion affects the bare steady state $\exp(-\Phi/D)$. The correction term $\tau(\nabla_i \Phi)^2/2$ is always positive, irrespective of the repulsive or attractive nature of the force $-\nabla_i \Phi$: it drives particles away from regions of large forces. The second correction term $-D\tau \nabla_i^2 \Phi$ is dominant for large values of D and can take either sign. It favors the presence of particles in convex potential landscapes. When the bare potential describes pairwise interactions, the corresponding effective potential contains three-body interactions stemming from the term $\tau(\nabla_i \Phi)^2/2$. Moreover, when Φ corresponds to repulsive interactions only, the associated Φ_{eff} combines repulsive and attractive interactions [38,40]. This captures how self-propulsion produces attractive effects out of repulsive forces, consistently with the enhanced tendency towards clustering reported experimentally for various colloidal systems [62–66].

It is interesting to note that similar functional forms to (17) and (18) are encountered in many contexts, from the semi-classical expansion of the Boltzmann distribution in powers of \hbar [67] to the Hermitian form of the Fokker-Planck operator [68]. It would be interesting to know whether this is just a coincidence or reflects the presence of a deeper connection.

B. One particle in one dimension

The systematic perturbative expansion presented in Sec. II can be carried out to any order in τ in the case of a single AOUP particle in $d = 1$ for an arbitrary smooth external potential Φ in an infinite space. In this case, the solvability conditions (14) admit a solution to arbitrary order n , explicitly given by

$$a^{(n-2,0)}(r) = \frac{1}{Z} \int_0^r dy e^{-\frac{\Phi(y)}{D}} \int_0^y dz e^{\frac{\Phi(z)}{D}} g_n(z), \quad (19)$$

where Z is a constant to be fixed by the normalization of the stationary measure. In this case, the solution can be obtained iteratively to arbitrary order, at the cost of expressions of increasing complexity. The result of this procedure is illustrated in Appendix A where we give the full stationary distribution $P_S(r, p)$ up to order τ^2 . Once the velocity is integrated out, we find

$$\begin{aligned} P_S(r) \sim & \exp \left[-\frac{\Phi}{D} + \tau \left(\Phi''(r) - \frac{\Phi'(r)^2}{2D} \right) \right. \\ & + \tau^2 \left(\frac{D\Phi^{(4)}(r)}{2} + \frac{\int^r \Phi'(y)^2 \Phi^{(3)}(y) dy}{2D} \right. \\ & \left. \left. - \Phi'(r)\Phi^{(3)}(r) - \frac{\Phi''(r)^2}{4} \right) + O(\tau^3) \right], \end{aligned}$$

where $\Phi^{(n)}$ refers to the n th-order derivative of Φ . Interestingly, this result is compatible with a recent, instanton-based derivation of the steady state of AOUPs obtained sending $D \rightarrow 0$ before taking the $\tau \rightarrow 0$ limit [69]. [Naturally, in this limit, only the terms proportional to D^{-1} in Eq. (20) survive.]

The case with periodic boundary condition is discussed in Appendix A. Furthermore, the perturbation expansion can also be generalized to the case of one particle in a central potential in arbitrary dimension, as well as to the case of two interacting particles with central forces. (We leave these cases to future works.)

Let us take advantage of working in a simpler, one-dimensional context to address more subtle questions regarding the nature of our small $\sqrt{\tau}$ expansion (7). It is for instance natural to ask whether this series admits a finite convergence radius in τ . Equation (7) indeed implicitly assumes that P_S is analytic in $\sqrt{\tau}$ which need not necessarily hold for any potential.

To address this question, we consider the potential $\Phi(x) = x^4/4$, at fixed D and for two different values of τ , and consider the marginal in space of the full distribution:

$$P_S(r) = \sum_n \bar{A}_n(r) \tau^n, \quad (20)$$

where $\bar{A}_n(r) = \int dv A_{2n}(r, v) \exp\{-\frac{1}{D}[\phi(x) + \frac{p^2}{2}]\}$ and A_{2n} is defined in (7). Truncating this series at order τ^8 , we show in Fig. 1(a) that the truncation seems well behaved for $\tau = 0.01$, yielding a precise quantitative agreement with the stationary distribution obtained numerically. Note that the distribution develops symmetric humps which highlight the non-Boltzmann nature of the stationary state. For $\tau = 0.2$, Fig. 1(c) shows that successive orders of the expansion are typical of an asymptotic series: each order in τ contributes a larger amount than the previous one with large positive and negative oscillations. This need not mean that the full series fails at capturing the steady state, but simply that finite sums yield poor approximations of the full series. An alternative procedure to estimate a series out of the asymptotic series of partial sums is to use Borel resummation. To do so, we use the method of Padé approximants. We begin by introducing the Borel transformed series

$$B_N(r, \tau) = \sum_{n=0}^N \frac{\bar{A}_n(r)}{n!} \tau^n \quad (21)$$

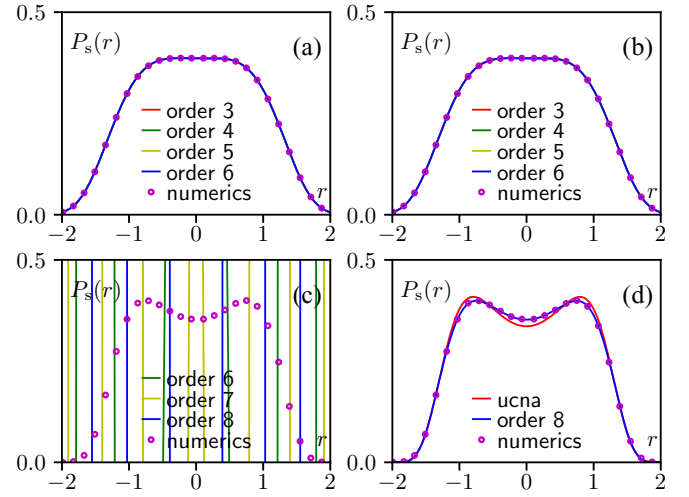


FIG. 1. Steady-state distribution of an AOUP in a confining potential $\Phi(x) = x^4/4$. Top: For $\tau = 0.01$, the series (20) converges rapidly and coincides with the numerics. The latter are obtained by integrating Eqs. (1) and (2) using the Heun algorithm (see [70] for detail). (a) The truncated Borel also describes correctly the data (b). Bottom: For $\tau = 0.2$, the series (20) is rapidly diverging and very far from the numerics (c). On the contrary, the truncated Borel sum describes very well the data (d).

and we approximate B_N as rational fractions $P_N(r, \tau) = \frac{Q_N(r, \tau)}{R_N(r, \tau)}$, where Q_N and R_N are polynomials in $\sqrt{\tau}$ of order N such that P_N and B_N coincide up to order τ^N . The series (20) can then be evaluated as the limit as $N \rightarrow \infty$ of $\hat{P}_N(r, \tau) \equiv \int_0^\infty dt P_N(r, t\tau) e^{-t}$, which is called the Borel resummation of the series (20) [71]. We first show in Fig. 1(b) that, when the series (20) is well approximated by its partial sum, it is (reassuringly) also well described by its truncated Borel sum. More interestingly, for $\tau = 0.2$, when the partial sums seem to diverge, the Borel resummation of (20) still agrees quantitatively with numerical estimates of the steady-state distribution, as shown in Fig. 1(d).

C. Approximate dynamics: Unified colored noise and Fox approximations

Approximate treatments of the dynamics (4) have been proposed in the past, based on schemes initially developed for noninteracting particles. They are usually referred to as the unified colored-noise approximation (UCNA) [54,55] and the Fox theory [52,53]. These approximations were first motivated by the description of the fluctuations of the radiation in the dye laser [55,72]. They have, in particular, been used to determine approximations of the stationary distribution of dynamics (4) and of mean first-passage times [73–76].

The UCNA consists in neglecting the left-hand side in Eq. (4):

$$\mathbb{M}_{i\alpha, j\beta} \dot{r}_{j\beta} = -\partial_{i\alpha} \Phi + (2D)^{1/2} \eta_{i\alpha}, \quad (22)$$

where $\partial_{i\alpha} = \partial/\partial r_{i\alpha}$, and we have introduced the tensor $\mathbb{M}_{i\alpha, j\beta} = \delta_{ij} \delta_{\alpha\beta} + \tau \partial_{i\alpha, j\beta}^2 \Phi$. As a result, the dynamics is now Markovian for the particle positions, at the cost of a position-dependent damping matrix \mathbb{M} . The derivation of

Eq. (22) yields an equation which is to be understood with the Stratonovich convention [76]. It follows that the associated Fokker-Planck equation for $P(\{\mathbf{r}_i\}, t)$ reads as

$$\partial_t P = \partial_{i\alpha} (P \mathbb{M}_{i\alpha, j\beta}^{-1} \partial_{j\beta} \Phi) + D \partial_{i\alpha} [\mathbb{M}_{i\alpha, j\beta}^{-1} \partial_{k\gamma} (\mathbb{M}_{k\gamma, j\beta}^{-1} P)], \quad (23)$$

where \mathbb{M}^{-1} denotes the inverse of \mathbb{M} . A simple derivation of the corresponding stationary distribution is detailed in Appendix B, and leads to [37,61]

$$P_S(\{\mathbf{r}_i\}) \sim \exp \left[-\frac{\Phi}{D} - \frac{\tau(\nabla_i \Phi)^2}{2D} \right] |\det \mathbb{M}|. \quad (24)$$

The stationary distribution differs from the equilibrium Boltzmann distribution $e^{-\Phi/D}$, which is recovered in the $\tau \rightarrow 0$ limit. The distribution (24) can be simplified to yield (18), showing it to coincide with our perturbative treatment to first order in τ . Note, however, that Appendix B shows that UCNA maps the AOUPs dynamics onto an *equilibrium one*, satisfying detailed balance with respect to the steady-state distribution (24). As such, it will be unable to capture any nonequilibrium dynamical effects, from the emergence of currents in ratchet potentials to nonvanishing entropy production.

The Fox theory uses projection methods to derive an approximate Fokker-Planck description of the dynamics of AOUPs [73,77]. In the spirit of this approach, we show in Appendix B that the approximate Fokker-Planck equation of N interacting AOUPs reads as, within the framework of Fox theory,

$$\partial_t P = \partial_{i\alpha} (P \partial_{i\alpha} \Phi) + D \partial_{i\alpha}^2 (\mathbb{M}_{i\alpha, j\beta}^{-1} P). \quad (25)$$

Note that this Fokker-Planck equation differs from that of [40], as commented by [78]. Again, both (25) and [40] approximate the dynamics of AOUPs by equilibrium processes, albeit with different space-dependent mobilities and diffusivities.

Comparing (25) with the UCNA (23) show both Fokker-Planck equations to share the same probability currents up to a multiplicative factor given by \mathbb{M}^{-1} . These two approximations thus yield the same stationary distribution (24), which agrees quantitatively with our perturbative result to first order in τ . However, both Fox and UCNA fail beyond this order. This may be seen directly by considering the order τ^2 for a particle in one dimension, for which UCNA and Fox predict

$$P_S(\{\mathbf{r}_i\}) \sim \exp \left[-\frac{\Phi}{D} - \frac{\tau(\Phi')^2}{2D} + \tau \Phi'' - \frac{\tau^2(\Phi'')^2}{2} + o(\tau^2) \right] \quad (26)$$

which differs from our systematic derivation presented in Sec. II B. Finally, we stress again that these approximation schemes both map the dynamics of AOUPs onto equilibrium ones and are thus unable to capture genuine nonequilibrium effects, unlike, as shown in Sec. IV, the expansion presented in Sec. II A.

D. Spatially varying activity

A marked difference between active and passive particles is that kinetic parameters, like the particle mobility, do not impact the steady-state distribution of passive particles, whereas they generically matter for active particles. The prototypical

example is that of a spatially dependent propulsion speed $v(\mathbf{r})$, which leads to a nonuniform distribution $P_s(\mathbf{r}) \propto \frac{1}{v(\mathbf{r})}$ for RTPs [23,33] and ABPs [33]. This result can be directly generalized to all self-propelled particles with spatially varying self-propulsion speeds and isotropic Markovian reorientation dynamics, whose master equation reads as [79]

$$\partial_t P(\mathbf{r}, \boldsymbol{\theta}) = -\nabla \cdot [v(\mathbf{r}) \mathbf{u}(\boldsymbol{\theta}) P(\mathbf{r}, \boldsymbol{\theta})] + \Theta P(\mathbf{r}, \boldsymbol{\theta}), \quad (27)$$

where $\boldsymbol{\theta}$ is a $d-1$ angular vector parametrizing the $d-1$ sphere in d spatial dimensions, $\mathbf{u}(\boldsymbol{\theta})$ the corresponding unit vector, and Θ is the operator accounting for the reorientation dynamics. Any isotropic reorientation process admits a uniform distribution over the sphere as a steady state. Up to normalization issue, $P(\mathbf{r}, \boldsymbol{\theta}) \propto \frac{1}{v(\mathbf{r})}$ is thus a steady-state solution of (27), which leads to a marginal in space $P_s(\mathbf{r}) \propto \frac{1}{v(\mathbf{r})}$. Note that this accumulation in slow regions remains valid in the presence of translational diffusion, but the precise form of the steady state now depends on the reorientation dynamics [34].

How this result generalizes to more complex dynamics of the self-propulsion velocity remains an open question. As we show below, AOUPs with position dependent $\tau(\mathbf{r})$ and $D(\mathbf{r})$ also generically have nonuniform steady states, which we characterize. We consider the following dynamics:

$$\begin{aligned} \dot{\mathbf{r}} &= \mathbf{v}, \\ \tau(\mathbf{r}) \dot{\mathbf{v}} &= -\mathbf{v} + \sqrt{2D(\mathbf{r})} \eta, \end{aligned} \quad (28)$$

where $\tau(\mathbf{r})$ and $D(\mathbf{r})$ are positive functions. The corresponding master equation for the probability density $P(\mathbf{r}, \mathbf{v}; t)$ is given by

$$\partial_t P(\mathbf{r}, \mathbf{v}; t) = -\nabla \cdot (\mathbf{v} P) + \nabla_{\mathbf{v}} \cdot \left(\frac{\mathbf{v}}{\tau} P + \frac{D}{\tau^2} \nabla_{\mathbf{v}} P \right). \quad (29)$$

Interestingly, introducing $\gamma \equiv \tau^{-1}$ and $T \equiv \frac{D}{\tau}$ maps this problem onto the dynamics of colloidal particles with inhomogeneous temperature and damping, a problem which has attracted a lot of attention in the past [80–85]. It is then a simple exercise to check that varying $\tau(\mathbf{r})$ and $D(\mathbf{r})$ while keeping $T = D/\tau$ uniform leads to a Maxwellian steady state $P_s(\mathbf{r}, \mathbf{v}) \propto \exp(-\frac{\mathbf{v}^2}{2T})$ and hence to a uniform distribution in position space $P_s(\mathbf{r})$. Under more general conditions, and somewhat surprisingly, Eq. (29) does not seem to admit simple steady-state solutions. As we show next, for slowly varying $\tau(\mathbf{r})$ and $D(\mathbf{r})$, one can nevertheless show the steady-state distribution to be given by $P_s(\mathbf{r}) \propto 1/T(\mathbf{r}) = \tau(\mathbf{r})/D(\mathbf{r})$.

Integrating (29) over \mathbf{v} leads to the continuity equation

$$\partial_t P(\mathbf{r}, t) = -\nabla \cdot \mathbf{j}(\mathbf{r}, t), \quad (30)$$

with $\mathbf{j}(\mathbf{r}, t) = \int d\mathbf{v} \mathbf{v} P(\mathbf{r}, \mathbf{v})$. Multiplying (29) by \mathbf{v} and integrating over \mathbf{v} then leads to

$$\partial_t \mathbf{j}(\mathbf{r}, t) = -\nabla \cdot \bar{\mathbf{q}}(\mathbf{r}, t) - \frac{1}{\tau(\mathbf{r})} \mathbf{j}(\mathbf{r}, t), \quad (31)$$

where $\bar{\mathbf{q}} = \int d\mathbf{v} (\mathbf{v} \otimes \mathbf{v}) P(\mathbf{r}, \mathbf{v})$ is a second-order tensor characterizing the local orientation field. Finally, the dynamics of

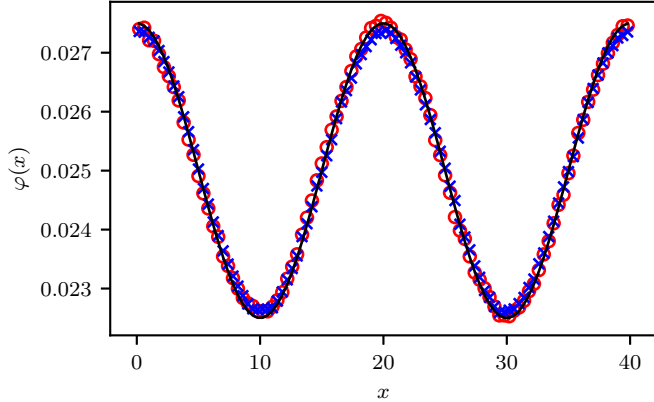


FIG. 2. Steady-state distributions of AOUPs evolving in 1D with $D = 1$ and $\tau(x) = 1 + \varepsilon \cos(4\pi x/L)$ (blue crosses) and with $\tau = 1$ and $D = [1 + \varepsilon \cos(4\pi x/L)]^{-1}$ (red circles), compared with the theoretical prediction (36) (black line). Parameters: $L = 40$, $\varepsilon = 0.1$

\bar{q} is given by

$$\begin{aligned} \partial_t \bar{q}_{\alpha\beta}(\mathbf{r}, t) &= -\nabla_\gamma \cdot \bar{\chi}_{\gamma\alpha\beta}(\mathbf{r}, t) - \frac{2\bar{q}_{\alpha\beta}(\mathbf{r}, t)}{\tau(\mathbf{r})} \\ &\quad + \frac{2D(\mathbf{r})P(\mathbf{r})\delta_{\alpha\beta}}{\tau(\mathbf{r})^2}, \end{aligned} \quad (32)$$

where $\bar{\chi} = \int d\mathbf{v}(\mathbf{v} \otimes \mathbf{v} \otimes \mathbf{v})P(\mathbf{r}, \mathbf{v})$ is a third-order tensor. As long as $\tau(\mathbf{r})$ is bounded, the fields $\bar{q}(\mathbf{r})$ and $\mathbf{j}(\mathbf{r})$ are slaved to the density $P(\mathbf{r})$ for timescales $t \gg \max[\tau(\mathbf{r})]$. On such timescales, assuming small gradients of $D(\mathbf{r})$ and $\tau(\mathbf{r})$, Eq. (32) leads to

$$\bar{q}_{\alpha\beta}(\mathbf{r}, t) = \frac{D(\mathbf{r})}{\tau(\mathbf{r})}P(\mathbf{r})\delta_{\alpha\beta} + O(\nabla). \quad (33)$$

In turn, this shows the local current to take the form

$$\mathbf{j}(\mathbf{r}, t) = -\tau(\mathbf{r})\nabla \left[\frac{D(\mathbf{r})}{\tau(\mathbf{r})}P(\mathbf{r}) \right] + O(\nabla^2). \quad (34)$$

Finally, this leads, to second order in gradient, to a diffusive dynamics for $P(\mathbf{r})$:

$$\partial_t P(\mathbf{r}, t) = \nabla \cdot \left[\tau(\mathbf{r})\nabla \left(\frac{D(\mathbf{r})}{\tau(\mathbf{r})}P(\mathbf{r}, t) \right) \right]. \quad (35)$$

Up to normalization issues, the steady state is then given by

$$P_s(\mathbf{r}, t) \propto \frac{\tau(\mathbf{r})}{D(\mathbf{r})} = \frac{1}{T(\mathbf{r})}. \quad (36)$$

Note that, in this approximation, the current \mathbf{j} vanishes in the steady state and \bar{q} is uniform in space: the spatial variations of the statistics of \mathbf{v} are compensated by those of $P_s(\mathbf{r})$. Equation (36) is illustrated numerically in Fig. 2. Equation (35) also shows that, on the timescales and space scales relevant to the fast variable treatments and to the gradient expansion, AOUPs evolving with dynamics (28) are equivalent to passive particles evolving under an Itô-Langevin dynamics

$$\dot{\mathbf{r}} = D(\mathbf{r})\nabla \log \tau(\mathbf{r}) + \sqrt{2D(\mathbf{r})}\eta. \quad (37)$$

Note that, without any approximation, Eq. (31) shows that, in the steady state, a spatially asymmetric periodic

modulation of $D(\mathbf{r})$ and $\tau(\mathbf{r})$ along one space direction cannot lead to a nonvanishing current. Consider indeed one-dimensional modulations of $D(\mathbf{r})$ and $\tau(\mathbf{r})$ along, say, the x direction. Equation (30) shows the current to be uniform in the steady state $\mathbf{j}(x) = \bar{j}\mathbf{u}_x$. By symmetry, Eq. (31) becomes

$$-\partial_x \bar{q}_{xx} = \frac{1}{\tau(x)}\bar{j}. \quad (38)$$

Integrating over one spatial period then leads to $\bar{j} = 0$ since $\tau^{-1}(x) > 0$ and q_{xx} is periodic. This is a surprising exception to the ratchet physics: breaking space and time symmetry may in more general cases lead to a vanishing current. Note that this extends to colloidal particles: an asymmetric modulation of the temperature along a single space direction does not lead to a steady current [80]. We stress that these results hold for noninteracting particles; pairwise forces may alter this conclusion, both for active [86] and passive particles [80].

III. MOTILITY-INDUCED PHASE SEPARATION

Motility-induced phase separation is a collective phenomenon observed in self-propelled particles whose self-propulsion is hindered at high density. The particles undergo a phase separation leading to the emergence of dense phases in the absence of attractive forces, at odds with the requirements for the emergence of cohesive phases in passive systems. MIPS has been reported in experiments on self-propelled colloids [10,64] and bacteria [87], where it led to a coexistence between dense arrested phases and a dilute, active, disordered gas. More recently, MIPS has been reported in a polar liquid [66] where a slowdown at high density led to the emergence of a dense macroscopic phase, which is reminiscent of traffic-jam physics [88–90].

Self-propelled particles with persistent, non-Gaussian noises have been shown to undergo MIPS when interacting via purely repulsive pairwise forces [24,64,91–93]. The resulting phase separation shares similarities with the one observed for particles interacting via quorum sensing, whose swimming speed depends on (and decreases with) the local density of particles [33,79,94]. These systems nevertheless display interesting differences in their mechanical and thermodynamical properties [58,95], in particular regarding the internal structure of the liquid phase [96–98]. A similar phase-separation scenario has been reported for AOUPs interacting via pairwise repulsive forces [41,99], as well as for resembling kinetic Monte Carlo dynamics [100,101]. This further highlights that, despite their simplicity, AOUPs retain the qualitative features of self-propelled particles at the level of collective dynamics, as was established, for instance, for the transition to collective motion [102]. In this section, we bring our knowledge on MIPS in AOUPs up to par with their non-Gaussian counterparts.

We derive in Sec. III A the collective hydrodynamics of N AOUPs interacting via pairwise repulsive forces and analyze MIPS in this context. We highlight the similarities with the case of non-Gaussian active particles. In particular, we show that the dynamics of the density field is driven by the divergence of a generalized stress tensor. Its scaling analysis can then be used to predict a linear instability at large enough

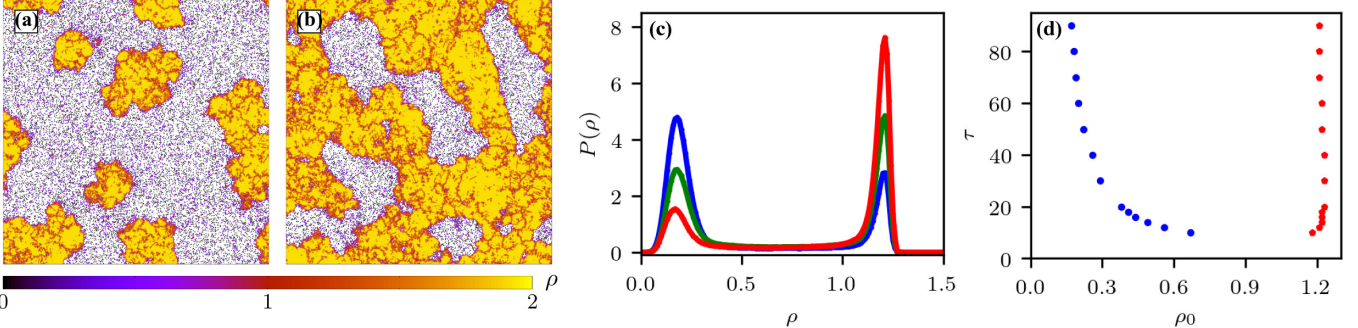


FIG. 3. Simulations of N AOUPs evolving with dynamics (40) and (41) and interacting via potential (39) in a 400×400 domain with periodic boundary conditions. Parameters: $D = 10$, $\varepsilon = r_0 = \mu = 1$. In (a) and (b), snapshots taken after a time $t = 10\,000$ show the occurrence of motility-induced phase separation for $\tau = 90$. The average densities are $\rho_0 = 0.5$ and $\rho_0 = 0.9$, respectively. Varying the overall density alters the size of the dense and dilute phases, but leaves their respective density unchanged. This can be seen from (c), which presents histograms of the local density measured in boxes of size 10×10 . The three curves correspond to $\rho_0 = 0.50, 0.70, 0.90$. Finally, the phase diagram shown in (d) is obtained by measuring the densities of the dilute and dense phases in simulations with an average density 0.9 and different values of τ . The densities are estimated from the maxima of histograms obtained as in (c).

persistence, which arises from the decrease of the flux of “active impulse,” a concept introduced in [103] and discussed in Sec. III A 1, as the local density of particles increases. Furthermore, an equation of state for the pressure of AOUPs interacting via pairwise forces can be established. Finally, as for ABPs and RTPs [64,95,104–107], a first-principles theory of the phase diagram of AOUPs interacting via pairwise forces remains an open problem. We then show in Sec. III B that AOUPs can also undergo MIPS due to quorum-sensing interactions, when the latter make their persistence times τ and noise amplitude D depend on the local density of particles. In practice, MIPS is seen when D/τ decreases sufficiently rapidly as the local density of particles increases.

A. Pairwise repulsive forces

We consider N AOUPs interacting via purely repulsive forces $\mathbf{f}_{ij} \equiv -\nabla_i V(\mathbf{r}_i - \mathbf{r}_j)$, where V is a pairwise Weeks-Chandler-Andersen (WCA) potential given by

$$V(r_{ij} = |\mathbf{r}_i - \mathbf{r}_j|) = \varepsilon \left[\left(\frac{r_0}{r_{ij}} \right)^{12} - \left(\frac{r_0}{r_{ij}} \right)^6 \right] + \frac{\varepsilon}{4}, \quad (39)$$

when $r_{ij} < 2^{1/6}r_0$ and $V = 0$ otherwise. The dynamics of the system reads as

$$\dot{\mathbf{r}}_i = \mathbf{v}_i + \mu \sum_j \mathbf{f}_{ij}, \quad (40)$$

$$\tau \dot{\mathbf{v}}_i = -\mathbf{v}_i + \sqrt{2D}\boldsymbol{\eta}_i. \quad (41)$$

For large enough τ , MIPS is observed and particles self-organize into dense arrested clusters which coexist with a dilute active gas (see Fig. 3).

1. Hydrodynamic equations and generalized stress tensor

To account for the underlying linear instability, we derive a hydrodynamic equation for the density field $\rho(\mathbf{r}, t)$, defined as

$$\rho(\mathbf{r}, t) = \langle \hat{\rho}(\mathbf{r}, t) \rangle \quad \text{with} \quad \hat{\rho}(\mathbf{r}, t) = \sum_{i=1}^N \delta[\mathbf{r} - \mathbf{r}_i(t)], \quad (42)$$

where the average is taken with respect to the realization of the microscopic noises $\boldsymbol{\eta}_i$. Following step by step the path laid out in [95] for ABPs, and thus omitting technical details, one finds that the dynamics of the density field is driven by the divergence of a current, which is given in terms of the divergence of a local “stress tensor” σ :

$$\dot{\rho} = -\nabla \cdot \mathbf{J}; \quad \mathbf{J} = \mu \nabla \cdot \sigma. \quad (43)$$

(The mechanical interpretation of σ is discussed in Sec. III A 3.) In noise-free, overdamped systems like the one considered here, the current in Eq. (43) is simply the particle mobility multiplied by the local force density. It may thus come as a surprise that the latter can be written as the divergence of a local tensor, despite the active, momentum-nonconserving nature of the particles.

Let us first note that the stress tensor can be split between an active and a passive part:

$$\sigma \equiv \sigma^{\text{act}} + \sigma^{\text{IK}}. \quad (44)$$

The contribution of the pairwise forces to the stress tensor is captured by $\sigma^{\text{IK}}(\mathbf{r})$, which was introduced by Irving and Kirkwood [108], and whose divergence is the local force density exerted at position \mathbf{r} :

$$\begin{aligned} \sigma_{\alpha\beta}^{\text{IK}}(\mathbf{r}) = & \frac{1}{2} \int d\mathbf{r}' \left\{ \frac{(\mathbf{r} - \mathbf{r}')_\alpha (\mathbf{r} - \mathbf{r}')_\beta}{|\mathbf{r} - \mathbf{r}'|} \frac{dV(|\mathbf{r} - \mathbf{r}'|)}{d|\mathbf{r} - \mathbf{r}'|} \right. \\ & \left. \times \int_0^1 d\lambda \langle \hat{\rho}[\mathbf{r} + (1 - \lambda)\mathbf{r}'] \hat{\rho}(\mathbf{r} - \lambda\mathbf{r}') \rangle \right\}. \end{aligned} \quad (45)$$

This formula can be derived by symmetrizing the force density $\sum_{i \neq j} \nabla_i V(\mathbf{r}_i - \mathbf{r}_j) = 1/2 \sum_{i \neq j} [\nabla_i V(\mathbf{r}_i - \mathbf{r}_j) - \nabla_j V(\mathbf{r}_i - \mathbf{r}_j)]$ and using that [109,110]

$$\delta(\mathbf{r} - \mathbf{r}_i) - \delta(\mathbf{r} - \mathbf{r}_j)$$

$$= -\nabla_{\mathbf{r}} \cdot \left[(\mathbf{r}_i - \mathbf{r}_j) \int_0^1 d\lambda \delta[\mathbf{r} - \mathbf{r}_i + \lambda(\mathbf{r}_i - \mathbf{r}_j)] \right]. \quad (46)$$

[This equality can be checked by series expanding in powers of λ and integrating over λ , which rebuilds the Taylor

expansion of $\delta(\mathbf{r} - \mathbf{r}_i) - \delta(\mathbf{r} - \mathbf{r}_i + \mathbf{r}_i - \mathbf{r}_j)$ in powers of $\mathbf{r}_i - \mathbf{r}_j$.] Note that, in a system translationally invariant along y , $\sigma_{xx}^{\text{IK}}(\mathbf{r})$ simply measures the force density along x exerted across an interface located at position \mathbf{r} , which endows Eq. (45) with a more direct physical interpretation.

The second contribution to the stress tensor $\sigma^{\text{act}}(\mathbf{r})$ is defined from

$$\nabla \cdot \sigma^{\text{act}}(\mathbf{r}) = \left\langle \sum_i \frac{\mathbf{v}_i}{\mu} \delta(\mathbf{r} - \mathbf{r}_i) \right\rangle. \quad (47)$$

Following again the path laid out in [95] then leads to

$$\sigma^{\text{act}}(\mathbf{r}) \equiv \left\langle \sum_i \frac{\mathbf{v}_i \tau}{\mu} \left[\mathbf{v}_i + \mu \sum_{j \neq i} \mathbf{f}_{ij} \right] \delta(\mathbf{r} - \mathbf{r}_i) \right\rangle \quad (48)$$

$$= \left\langle \sum_i \dot{\mathbf{r}}_i \frac{\mathbf{v}_i \tau}{\mu} \delta(\mathbf{r} - \mathbf{r}_i) \right\rangle. \quad (49)$$

Equation (49) provides a simple interpretation to $\sigma^{\text{act}}(\mathbf{r})$: An AOUP whose self-propulsion force is \mathbf{v}_i/μ at time t receives an average momentum $\tau \mathbf{v}_i/\mu$ from the substrate in the future, called its “active impulse” [103]. The underlying physical picture is that the active impulse measures the active force “stock” of the particles. In Eq. (49), $\sigma^{\text{act}}(\mathbf{r})$ thus measures the flux of active impulse through the medium due to the motion of the particles, much like for ABPs and RTPs [103]. Equation (47) then expresses that any nonvanishing active force exerted in a volume results from the difference between inward and outward fluxes of active impulse, which measures what has been “spent” to maintain a nonzero steady force.

The hydrodynamic equation (43), together with the expressions (45) and (49) for σ^{IK} and σ^{act} , can be used both to predict the instability of a homogeneous system at large enough persistence, as detailed in Sec. III A 2, and to show the existence of an equation of state for the pressure, as discussed in Sec. III A 3.

2. Scaling analysis and linear instability

To proceed, it is natural to assume, following [111], that the stress tensor $\sigma(\mathbf{r})$ is well approximated by a local equation of state $\sigma(\rho(\mathbf{r}))$. Consider a small periodic perturbation $\delta\rho_q$, say along the x direction, around a mean density ρ_0 . Equation (43) shows it to evolve as $\partial_t \delta\rho_q = -q^2 \mu \sigma'(\rho_0) \delta\rho_q$ so that $\sigma'(\rho_0) < 0$ signals the onset of a linear instability and defines a spinodal region. To proceed further, one could approximate the various components of σ using local equations of states $\sigma^{\text{IK}}(\rho)$, $\sigma^{\text{act}}(\rho)$, as was done for ABPs [111]. However, direct inspection of their physical origin already captures most of the physics.

Much like for purely repulsive passive particles, $\sigma^{\text{IK}}(\rho_0)$ vanishes in the low-density, noninteracting limit and increases monotonously until it diverges at close packing [112]. Because particles stop when the interparticle force balances the propulsive one, the scale of \mathbf{f}_{ij} is set by v_0/μ , where $v_0 = \sqrt{D/\tau}$ is the typical scale of the self-propulsion speed. The integral in (45) then selects the typical interaction length r_0

and the overall scaling of σ^{IK} is

$$\sigma^{\text{IK}}(\rho_0) \sim \rho_0 \sqrt{\frac{D}{\tau} \frac{r_0}{\mu}} S, \quad (50)$$

where the dependence on ρ_0 has been formally written, for dimensional reasons, as $\rho_0 S$, where S is a dimensionless scaling function of the rescaled density [111]. (Below a crowding density ρ_c , S is well approximated by a linearly decaying function $S = 1 - \rho/\rho_c$ [24,58,95,113].) Note that (50) can be derived using (45) or, equivalently, using the Virial-type formula $\sigma^{\text{IK}} \sim \langle \sum_{i \neq j} (\mathbf{r}_i - \mathbf{r}_j) \otimes \nabla_i V(\mathbf{r}_i - \mathbf{r}_j) \rangle$ [114,115].

Contrary to σ^{IK} , $\sigma^{\text{act}}(\rho_0)$ is expected to be a non-monotonous function of ρ_0 . It first increases linearly with the density until interactions kick in. Because active particles collide more often with particles lying ahead than behind [113], the main effect of these interactions is to *lower* the flux of active impulse as the density increases, until it vanishes at close packing, leading to a nonmonotonous variation of σ^{act} . Inspection of Eq. (49) shows the typical scale of σ^{act} to be

$$\sigma^{\text{act}} \sim \rho_0 \frac{v_0^2 \tau}{\mu} \tilde{S}(\rho_0) = \rho_0 \frac{D}{\mu} \tilde{S}, \quad (51)$$

where $\tilde{S}(\rho)$ is another dimensionless scaling function.

An overall decreasing stress tensor can then be observed when the decrease of $\sigma^{\text{act}}(\rho_0)$ is strong enough to compensate the increase of $\sigma^{\text{IK}}(\rho_0)$. From Eqs. (50) and (51), this is realized when the rescaled persistence length is large enough:

$$\ell_p = \frac{\sqrt{D\tau}}{r_0} \gg \frac{S}{\tilde{S}}. \quad (52)$$

Let us highlight, once again, the similarity of this criterion with that obtained for ABPs or RTPs [111].

3. An equation of state for pressure

Finally, before turning to quorum-sensing interactions, let us note that, as for other active particles interacting via pairwise forces [95], the analogy between σ and a stress tensor goes further than Eq. (43): it has a direct mechanical interpretation. Confining AOUPs by an external potential V_w indeed leads to

$$\mathbf{J}(\mathbf{r}) = \mu \nabla \cdot [\sigma^{\text{act}}(\mathbf{r}) + \sigma^{\text{IK}}(\mathbf{r})] - \mu \rho \nabla V_w \quad (53)$$

with σ^{IK} and σ^{act} given by (45) and (49). In a flux-free steady state, Eq. (53) shows the force density exerted by the particles on the confining boundary $\rho \nabla V_w$ to be given by the divergence of the stress tensor σ . Consider a confining boundary parallel to \hat{e}_y . Integrating (53) from a point \mathbf{r}_{bulk} , deep in the bulk of the system, to infinity along \hat{e}_x shows the mechanical pressure exerted by the particles on the wall, $P = \int_{x_{\text{bulk}}}^{\infty} \rho(x, y) \partial_x V_w dx$, to be given by $P = -\sigma_{xx}(\mathbf{r}_{\text{bulk}})$. In a bulk phase-separated system, x_{bulk} can be equally chosen in any of the phases, showing that the pressure is identical in either of the coexisting phases.

B. Quorum-sensing interactions

From bacteria to self-propelled Janus colloids, many active particles experience propelling forces whose statistics depend on the composition of their environment and may thus be

altered by the presence of other nearby active particles. Such mediated interactions, whether chemical, hydrodynamic or metabolic, can be modeled, somewhat crudely, by quorum-sensing (QS) interactions. These can be described using a self-propulsion whose characteristics depend on the density of neighboring particles. Consider the dynamics of ABP or RTP, $\dot{\mathbf{r}} = v\mathbf{u}(\theta)$, where θ undergoes either rotational diffusion or a Poisson jump process, respectively. Quorum-sensing interactions can be modeled by considering a self-propulsion speed that is both a function of the position of the particle \mathbf{r} and a functional of the density field $\hat{\rho}$: $v = v(\mathbf{r}, [\hat{\rho}])$ [94,95,116]. In this context, a homogeneous phase at density ρ_0 has been shown to be linearly unstable to MIPS whenever [33,34,79]

$$\frac{d}{d\rho_0} \log[v(\rho_0)] < -\frac{1}{\rho_0}, \quad (54)$$

where $v(\rho_0)$ is the self-propulsion speed $v(\mathbf{r}, [\hat{\rho}])$ of a particle in a homogenous system at density ρ_0 . The role of QS for AOUPs with varying propulsion speed has not been studied so far. To fill this gap, we consider N AOUPs, whose dynamics is given by $\dot{\mathbf{r}}_i = \mathbf{v}_i$ and

$$\tau(\mathbf{r}_i, [\hat{\rho}])\dot{\mathbf{v}}_i = -\mathbf{v}_i + \sqrt{2D(\mathbf{r}_i, [\hat{\rho}])}\boldsymbol{\eta}_i, \quad (55)$$

where τ and D are functions of \mathbf{r} and functionals of the density field $\hat{\rho}(\mathbf{r})$. In practice, we choose $\tau(\mathbf{r}, [\hat{\rho}]) = \tau(\tilde{\rho}(\mathbf{r}))$ and $D(\mathbf{r}, [\hat{\rho}]) = D(\tilde{\rho}(\mathbf{r}))$ where $\tilde{\rho}(\mathbf{r})$ is a local smooth density field felt by a particle at position \mathbf{r} . It is defined through

$$\tilde{\rho}(\mathbf{r}) = \int d\mathbf{r}' K(\mathbf{r} - \mathbf{r}')\hat{\rho}(\mathbf{r}'), \quad (56)$$

with $K(\mathbf{r})$ a positive, symmetric kernel, normalized by $\int d\mathbf{r} K(\mathbf{r}) = 1$ and with a typical range ℓ_0 .

1. A diffusive fluctuating hydrodynamics

We consider a long-time, large system-size limit in which the density field evolves over timescales $t \propto L^z$, where z is the corresponding dynamical exponent, so that there is a clear separation between the persistence time τ and the timescale of the evolution of the density field. We thus assume that the dynamics of particle i is well described by its diffusive approximation. Using (37), this is given by

$$\dot{\mathbf{r}}_i = D(\tilde{\rho}(\mathbf{r}_i))\nabla \log[\tau(\tilde{\rho}(\mathbf{r}_i))] + \sqrt{2D(\tilde{\rho}(\mathbf{r}_i))}\boldsymbol{\eta}_i. \quad (57)$$

Equation (57) amounts to a diffusive approximation of the dynamics of the N interacting AOUPs by coupled Langevin dynamics. Standard methods of stochastic calculus [79,94,117] then allow one to derive a stochastic evolution equation for $\hat{\rho}$. Altogether, the fluctuating hydrodynamics of N interacting AOUPs is given by

$$\partial_t \hat{\rho}(\mathbf{r}, t) = \nabla \cdot \left[D\nabla \hat{\rho} + \hat{\rho}\tau \nabla \left(\frac{D}{\tau} \right) + \sqrt{2D\hat{\rho}}\Lambda(\mathbf{r}, t) \right], \quad (58)$$

where $\Lambda(\mathbf{r}, t)$ is a Gaussian white-noise field of zero mean and unit variance.

2. Linear stability analysis of the mean-field hydrodynamics

Equation (58) is the main result of this section: it provides the fluctuating hydrodynamics of N AOUPs interacting via

QS through $D(\tilde{\rho})$ and $\tau(\tilde{\rho})$. The structure of this equation is very similar to that of RTPs and ABPs interacting via density-dependent self-propulsion speed [79], but the relationship between the macroscopic transport parameters and the microscopic parameters of the self-propulsion is clearly different. The methods developed to study the collective behaviors of RTPs and ABPs interacting via QS [95,118] can be directly generalized to AOUPs. First, Eq. (58) immediately leads to an exact evolution equation for the mean density field $\rho(\mathbf{r}, t)$ through

$$\partial_t \rho(\mathbf{r}, t) = \nabla \cdot \left[\left(D(\mathbf{r}, [\hat{\rho}])\nabla \hat{\rho} + \hat{\rho}\tau(\mathbf{r}, [\hat{\rho}])\nabla \left(\frac{D(\mathbf{r}, [\hat{\rho}])}{\tau(\mathbf{r}, [\hat{\rho}])} \right) \right) \right]. \quad (59)$$

Note that this equation is neither closed, nor local. A further simplifying step is to implement a mean-field approximation and replace $\langle f(\mathbf{r}, [\hat{\rho}]) \rangle$ by $f(\mathbf{r}, [\rho])$, yielding

$$\partial_t \rho(\mathbf{r}, t) = \nabla \cdot \left[D(\mathbf{r}, [\rho])\nabla \rho + \rho\tau(\mathbf{r}, [\rho])\nabla \left(\frac{D(\mathbf{r}, [\rho])}{\tau(\mathbf{r}, [\rho])} \right) \right]. \quad (60)$$

At this stage, Eq. (60) already allows one to predict the onset of a linear instability leading to MIPS. This is done by computing the linear dynamics of a perturbation $\delta\rho(\mathbf{r}, t) \equiv \rho(\mathbf{r}, t) - \rho_0$ around a homogeneous profile $\rho(\mathbf{r}, t) = \rho_0$, leading to

$$\partial_t \delta\rho(\mathbf{r}, t) = D(\rho_0)\Delta\delta\rho + \rho_0\tau(\rho_0)\left(\frac{D(\rho_0)}{\tau(\rho_0)}\right)' \Delta\delta\rho, \quad (61)$$

where $\Delta = \nabla^2$, the prime refers to a derivative with respect to ρ_0 , and we defined $D(\rho_0) \equiv D(\mathbf{r}, [\rho_0])$ and similarly for $\tau(\rho_0)$. A Fourier transform then shows that mode q relaxes with rate Λ_q , where

$$\Lambda_q = D(\rho_0)q^2 \left[1 + \rho_0 \log \left(\frac{D(\rho_0)}{\tau(\rho_0)} \right)' \right]. \quad (62)$$

The mode is unstable whenever $\Lambda_q < 0$, hence the instability criterion

$$\left(\log \frac{D(\rho_0)}{\tau(\rho_0)} \right)' < -\frac{1}{\rho_0}. \quad (63)$$

Equation (63) defines the spinodal region of AOUPs interacting via quorum sensing; it is the direct counterpart for AOUPs of the standard MIPS criterion (54) derived for ABPs and RTPs.

Note that Eq. (63) predicts a density-dependent persistence time to lead to MIPS whenever $\rho_0\tau'(\rho_0) > \tau(\rho_0)$ whereas density-dependent tumbling rates or rotational diffusion, which control the persistence times of ABPs and RTPs, do not lead to any interesting collective behaviors. The MIPS experienced by AOUPs interacting via such a density-dependent persistence time is illustrated in Fig. 4.

3. Phase diagram

The full phase diagram of ABPs and RTPs interacting via quorum-sensing interactions has recently been predicted analytically by carrying out one more approximation step

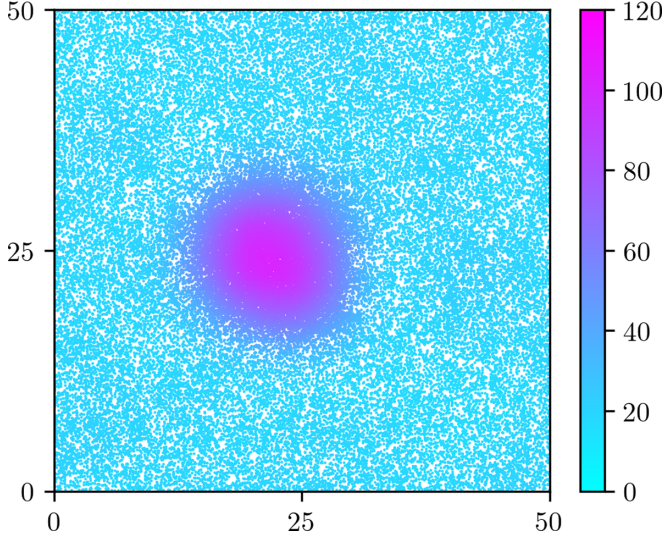


FIG. 4. Snapshots of N AOUPs interacting via quorum sensing through Eq. (55) with $\tau = 1$ and $D(\mathbf{r}, [\rho]) = D_0 e^{-\lambda \phi} \arctan(\tilde{\rho}(\mathbf{r})/\phi)$. The field $\tilde{\rho}(\mathbf{r})$ measures the density field $\hat{\rho}$ averaged over a disk of radius 1 centered in \mathbf{r} . A linear instability will lead to MIPS whenever $\lambda\phi > 2$, according to Eq. (63). Simulation parameters: $D_0 = 1$, $\rho_0 = N/L^2 = 25$, $L = 50$, $\lambda = 0.05$, $\phi = 44.72$, so that $\lambda\phi = 2.23$. Color encodes the density averaged over a disk of radius 5. Starting from a random initial condition, the snapshot is taken after a time $t = 49\,800$.

[95,118]. We present here a direct application of this method to AOUPs. We first recast (60) into

$$\partial_t \rho(\mathbf{r}, t) = \nabla \cdot [\rho D(\mathbf{r}, [\rho]) \nabla g(\mathbf{r}, [\rho])], \quad (64)$$

$$g(\mathbf{r}, [\rho]) = \log \rho + \log \frac{D(\mathbf{r}, [\rho])}{\tau(\mathbf{r}, [\rho])}. \quad (65)$$

Equation (64) shows that $g(\mathbf{r}, [\rho])$ acts as a chemical potential. Using a second-order gradient expansion, the nonlocal sampling of the density field through the kernel $K(\mathbf{u})$ can be written as

$$\langle \tilde{\rho}(\mathbf{r}) \rangle \simeq \rho(\mathbf{r}) + \frac{1}{2} \ell_0^2 \Delta \rho(\mathbf{r}), \quad (66)$$

where $\ell_0^2 = \int \mathbf{u}^2 K(\mathbf{u}) d\mathbf{u}$. This allows us to expand $g(\mathbf{r}, [\rho])$ into

$$g(\mathbf{r}, [\rho]) = g_0(\rho(\mathbf{r})) - \kappa(\rho(\mathbf{r})) \Delta \rho(\mathbf{r}), \quad (67)$$

where

$$g_0(\rho) = \log \rho + \log \frac{D(\rho)}{\tau(\rho)}, \quad (68)$$

$$\kappa(\rho) = \frac{\ell_0^2}{2} \left(\frac{\tau'(\rho)}{\tau(\rho)} - \frac{D'(\rho)}{D(\rho)} \right). \quad (69)$$

Following the method laid out in [95,118], one introduces the change of variable $R(\rho)$, solution of $R'(\rho) = \frac{1}{\kappa(\rho)}$. This allows us to write

$$g(\mathbf{r}) = -\frac{\delta \mathcal{F}(R)}{\delta R(\mathbf{r})}, \quad (70)$$

where $\mathcal{F}[R] = \int d\mathbf{r} [\phi(R) + \frac{\kappa}{2R'} (\nabla R)^2]$ is the generalized free energy whose local density is such that

$$\frac{d\phi(R)}{dR} = g_0(\rho(R)). \quad (71)$$

The phase diagram can then be predicted, at this diffusive, mean-field level, by carrying out a common-tangent construction on $\phi(R)$. This was shown in [95,118] to give quantitative agreement with microscopic simulations as soon as ℓ_0 is large enough that each particle interacts with many of its neighbors.

IV. EMERGENCE OF TIME-REVERSAL SYMMETRY BREAKING

In this section, we discuss observables which can be used to measure the deviation from equilibrium of AOUPs. First, we consider the particle current which arises spontaneously when introducing an external asymmetric potential. We obtain its expression to leading order based on the small-persistence-time expansion detailed in Sec. II. Then, we derive the entropy production rate quantifying the breakdown of time-reversal symmetry [119]. This observable has been used extensively as an unambiguous nonequilibrium signature in systems driven by external fields [120–124] and it has attracted a lot of attention recently in the field of active matter [41,45,125–135]. Finally, we end by discussing the symmetry of time correlations and its relation to entropy production.

A. Current and ratchet

Nonequilibrium systems can sustain currents in the steady state. One of the simplest settings for this to happen is a stochastic ratchet: a fluctuating nonequilibrium dynamics in a spatially asymmetric potential landscape generically leads to nonvanishing currents in the steady state [136,137]. Recently, several works considered active particles in asymmetric landscapes, both experimentally [27–29,138,139] and theoretically [26,31,86,140–142].

We consider here a single AOUP on a ring of length L in an asymmetric potential of period L . Our interest goes to the induced current $J = \langle p \rangle$ in the steady state. An interesting spinoff of our computation of the stationary measure detailed in Sec. II B and Appendix A is a perturbative expression for J . To leading order in τ , J reads as

$$J = \langle p \rangle = \tau^2 \frac{L \int_0^L \Phi'(r)^2 \Phi^{(3)}(r) dr}{2 \int_0^L e^{\frac{\Phi}{\tau}} dr \int_0^L e^{-\frac{\Phi}{\tau}} dr} + o(\tau^2). \quad (72)$$

We compare in Fig. 5 the above prediction with the results of numerical simulations of an AOUP experiencing a potential $\Phi(r) = \sin(\pi r/2) + \sin(\pi r)$. The agreement between our numerical simulations and Eq. (72) confirms the validity of our approximation at small τ . In particular, this is an effect that could not be captured by the UCNA or Fox approximations described in Sec. II C: both would predict $J = 0$.

B. Entropy production rate

To probe quantitatively the nonequilibrium properties of the dynamics, we now consider the entropy production rate S [119,123]. It is defined as the rate of (Kullback-Leibler)

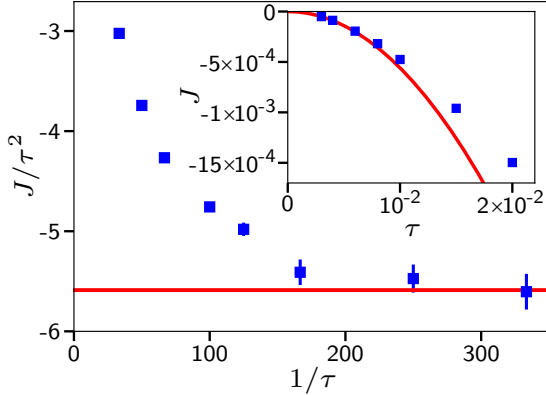


FIG. 5. Plot of the normalized current J/τ^2 induced by a ratchet potential $\Phi(r) = \sin(\pi r/2) + \sin(\pi r)$ as a function of the inverse of the persistence time τ^{-1} . The blue dots correspond to numerical simulations with error bars given by the standard deviation; the red line is our analytical prediction in the small τ limit obtained from Eq. (72). In the inset, we plot J as a function of τ .

divergence between the probability weights associated with a given realization of the dynamics $\{\mathbf{r}_i(t), \mathbf{p}_i(t)\}$, and its time-reversed counterpart $\{\mathbf{r}_i^R(t), \mathbf{p}_i^R(t)\}$, respectively denoted by \mathcal{P} and \mathcal{P}^R , as

$$\mathcal{S} = \lim_{t_f \rightarrow \infty} \frac{1}{t_f} \left\langle \ln \frac{\mathcal{P}[\{\mathbf{r}_i(t), \mathbf{p}_i(t)\}]}{\mathcal{P}^R[\{\mathbf{r}_i^R(t), \mathbf{p}_i^R(t)\}]} \right\rangle, \quad (73)$$

where t_f is the length of the trajectory. The entropy production rate \mathcal{S} quantifies the irreversibility of the dynamics. Using standard path-integral formalism [143], the trajectory weight can be written as $\mathcal{P} \sim e^{-\mathcal{A}}$, where the dynamic action \mathcal{A} reads as

$$\mathcal{A} = \frac{1}{4D} \int_0^{t_f} [\tau \dot{\mathbf{p}}_i + \mathbf{p}_i + (1 + \tau \mathbf{p}_j \cdot \nabla_j) \nabla_i \Phi]^2 dt. \quad (74)$$

We define the reversed trajectories $\{\mathbf{r}^R, \mathbf{p}^R\}$ in terms of the forward ones as

$$\mathbf{r}_i^R(t) = \mathbf{r}_i(t_f - t), \quad \mathbf{p}_i^R(t) = -\mathbf{p}_i(t_f - t). \quad (75)$$

Note that this amounts to comparing a forward trajectory with a backward one, realized by a particle whose initial velocity is the opposite of the final velocity of the forward trajectory, a choice which has been debated [128,132].

From this definition, we deduce the action difference $\delta\mathcal{A} = \mathcal{A} - \mathcal{A}^R$ as

$$\begin{aligned} \delta\mathcal{A} = & \frac{1}{D} \int_0^{t_f} \{\mathbf{p}_i \cdot \nabla_i \Phi + \tau [\dot{\mathbf{p}}_i \cdot \mathbf{p}_i + \nabla_i \Phi \cdot (\mathbf{p}_j \cdot \nabla_j) \nabla_i \Phi] \\ & + \tau^2 \dot{\mathbf{p}}_i \cdot (\mathbf{p}_j \cdot \nabla_j) \nabla_i \Phi\} dt, \end{aligned} \quad (76)$$

where $\mathcal{A}^R = \mathcal{A}(\mathbf{r}_i^R(t), \mathbf{p}_i^R(t))$ and we use the Stratonovich convention. Using $\mathbf{p}_i = \dot{\mathbf{r}}_i$, it appears that the first line in (76) integrates into a finite contribution $[\Phi + \tau \mathbf{p}^2/2 + \tau(\nabla \Phi)^2/2]_0^{t_f}$, which does not contribute to \mathcal{S} as $t_f \rightarrow \infty$. We assume that the time and ensemble averages coincide under the ergodicity condition, leading us to express the entropy production rate as

$$\mathcal{S} = -\frac{\tau^2}{D} \langle (\dot{\mathbf{p}}_i \cdot \nabla_i)(\mathbf{p}_j \cdot \nabla_j) \Phi \rangle. \quad (77)$$

Using the chain rule

$$\frac{d}{dt} \langle (\mathbf{p}_i \cdot \nabla_i)^2 \Phi \rangle = 2 \langle (\dot{\mathbf{p}}_i \cdot \nabla_i)(\mathbf{p}_j \cdot \nabla_j) \Phi \rangle + \langle (\mathbf{p}_i \cdot \nabla_i)^3 \Phi \rangle, \quad (78)$$

and given that $d\langle A \rangle/dt$ vanishes in steady state for any observable A , we then deduce

$$\mathcal{S} = \frac{\tau^2}{2D} \langle (\mathbf{p}_i \cdot \nabla_i)^3 \Phi \rangle. \quad (79)$$

The entropy production rate vanishes when Φ is quadratic, a case which has attracted interest in the past [36]. In such a harmonic trap, AOUPs have a Gaussian, Boltzmann-type distribution, albeit with a potential-dependent “temperature.” Equation (79) shows that this quantitative difference with thermal equilibrium does not imply a breakdown of time-reversal symmetry, in the sense that detailed balance holds. The anharmonicity of the potential can thus be used as a handle to drive AOUPs out of equilibrium. Note that we use \mathcal{S} solely to detect a breakdown of time-reversal symmetry. It can also be granted a more traditional thermodynamical meaning, as recently discussed in [31,131,144].

Equation (79) is a global measure of the entropy production rate over the whole system. We now turn to a more detailed study of how this entropy is locally produced and, more precisely, of the spatial structures which are most sensitive to time-reversal symmetry breaking.

C. Entropy production in MIPS

The relationship between MIPS and equilibrium phase-separation was initially suggested in [33], using a coarse-grained description only valid at the homogeneous level. Further discussions on the role of gradient terms has led to the realization that this mapping onto equilibrium is generically broken at higher order in gradients [18,95,96,145,146]. The entropy production of active field theories was indeed shown to be peaked at interfaces between coexisting phases [147], a result which begs to be tested in particle models.

To do so, we first construct a map of entropy production rate starting from the global formula (79) for \mathcal{S} . We consider the case where particles interact through a pair potential:

$$\Phi = \frac{1}{2} \sum_{i,j=1}^N V(\mathbf{r}_i - \mathbf{r}_j), \quad (80)$$

where $V(0) = 0$ to avoid self-interaction. To rewrite (79) as a sum over particle contributions, we first note that

$$\begin{aligned} & \langle (\mathbf{p}_i \cdot \nabla_i)^3 \Phi \rangle \\ &= \frac{1}{2} \sum_{n,p,q,i,j=1}^N \langle (\mathbf{p}_n \cdot \nabla_n)(\mathbf{p}_p \cdot \nabla_p)(\mathbf{p}_q \cdot \nabla_q) V(\mathbf{r}_i - \mathbf{r}_j) \rangle. \end{aligned} \quad (81)$$

Using that

$$\sum_k (\mathbf{p}_k \cdot \nabla_k) V(\mathbf{r}_i - \mathbf{r}_j) = (\mathbf{p}_i - \mathbf{p}_j) \cdot \nabla_i V(\mathbf{r}_i - \mathbf{r}_j) \quad (82)$$

the entropy production rate can be rewritten as

$$\mathcal{S} = \sum_{i=1}^N \sigma_i, \quad (83)$$

where σ_i is given by

$$\sigma_i = \left\langle \frac{\tau^2}{4D} \sum_{j=1}^N [(\mathbf{p}_i - \mathbf{p}_j) \cdot \nabla_i]^3 V(\mathbf{r}_i - \mathbf{r}_j) \right\rangle. \quad (84)$$

Equations (83) and (84) split the total entropy production rate into a sum of particle contributions. It is thus tempting to refer to σ_i as the entropy production rate of particle i . Note, however, that we have proven neither that σ_i is positive nor that the decomposition (84) is unique. This interpretation thus has to be taken with a pinch of salt.

Our aim is to compute the local rate of entropy production associated with a phase-separated set of AOUPs, and in particular investigate the correlation between the structure of the density field and entropy production. We consider N particles in a $2d$ box, interacting via a short-range soft-core potential of the form

$$V(\mathbf{r}) = \varepsilon \exp \left[-\frac{1}{(r/a)^2 - 1} \right] \quad (85)$$

for $r \leq a$. As discussed in Sec. III A, such pairwise repulsive forces can lead to phase separation at high enough persistence: a macroscopic cluster of particles then forms and slowly diffuses in the system. This slow diffusion makes the comparison between the average density and the entropy production rate profiles numerically difficult and we thus pin the center of the cluster by applying a truncated harmonic trap of the form $U(\mathbf{r}) = U_0(r/a_0)^2$ for $r \leq a_0$. Note that the harmonic trap does not directly contribute to the entropy production since it is harmonic.

As shown in Fig. 6 for different particle densities, a macroscopic cluster of particles indeed localizes in the center of the system and coexists with a surrounding dilute gas phase. Increasing the density mostly results in a shift of the boundary between the two phases as the cluster grows. Using Eq. (84), the contribution of each particle to the entropy production can be measured: particles in the bulk of each phase have negligible contributions whereas those localized at the boundary of the cluster exhibit large values, both positive and negative, of σ_i . To compute the net contribution to the entropy production, we construct a density $\bar{\sigma}(r) = \overline{\sum_{i=1}^N \sigma_i \delta(r - r_i)}$ of entropy production rate, where the overbar represents a binning procedure and a time average in the steady state. The resulting profiles are shown in Fig. 7, where they are compared to the density profiles.

As hinted from Fig. 6, $\sigma(r)$ is indeed much smaller in bulk phases than at the boundary of the dense cluster, which highlights that the breakdown of time-reversal symmetry in MIPS is dominated by interface physics. Novelty with respect to a *bona fide* equilibrium phase separation will thus mostly operate at the interface between dilute and dense phases, which echoes recent results on reversed Ostwald ripening and bubbly phase separations in active systems [96,148]. The almost negligible value of σ_i in both bulk phases can be understood by inspection of (84): σ_i vanishes in the dense phase since the

relative velocities between the particles vanish, and it reaches a small plateau value in the dilute phase, where collisions are scarce. On the contrary, $\sigma(r)$ reaches a maximum value at the interface where fast particles coming from the dilute phase collide onto slow ones arrested in the crowded cluster.

Note that our microscopic analysis corroborates the phenomenological coarse-grained approach of [147]. This validates *a posteriori* the idea that, at the coarse-grained scale, the difference between MIPS and an equilibrium phase separation lies in nonconservative gradient terms contributing mostly at the interface. Finally, the differences between all microscopic models exhibiting MIPS-like behaviors, whether on or off lattice, interacting via quorum-sensing or pairwise forces, should be mostly apparent, at the coarse-grained scale, in the different types of gradient terms they will generate.

D. Symmetry of time correlations

While entropy production rate provides a formal estimate of the breakdown of time-reversal symmetry, its practical significance may be hard to grasp. It is furthermore not easily accessible experimentally, and its measurement has thus been carried out mostly on low-dimensional systems [149,150]. A more pragmatic measurement of irreversibility can be inferred from the asymmetry of time correlations of physical observables. For systems in equilibrium, time reversibility indeed implies that time correlations are symmetric. Consider first an overdamped equilibrium system whose configurations are specified by the positions $\mathbf{r} = \{\mathbf{r}_i\}$ of the particles. For any two observables $A(\mathbf{r})$ and $B(\mathbf{r})$, time reversibility implies that

$$\langle A(0)B(t) \rangle - \langle A(t)B(0) \rangle = 0, \quad (86)$$

where the average is defined as

$$\langle A(0)B(t) \rangle \equiv \int d\mathbf{r} P_s(\mathbf{r}) A(\mathbf{r}) e^{t\mathcal{L}^\dagger} B(\mathbf{r}). \quad (87)$$

In (87), \mathcal{L} is the Fokker-Planck operator and $P_s(\mathbf{r})$ the corresponding steady-state distribution.

Equation (86) can be generalized to systems with odd variables under time reversal ($\mathbf{p} = \{\mathbf{p}_i\}$), such as, for instance, underdamped dynamics. As discussed in Appendix C, considering observables $A = A(\mathbf{r}, \mathbf{p})$ and $B = B(\mathbf{r}, \mathbf{p})$, time reversibility now implies that

$$\Delta_{A,B}(t) \equiv \langle A(0)B(t) \rangle - \langle (\Pi A)(t)(\Pi B)(0) \rangle = 0, \quad (88)$$

where $\Pi A(\mathbf{r}, \mathbf{p}) = A(\mathbf{r}, -\mathbf{p})$ and analogously for B . In Eq. (88), the average is defined as in (87), albeit with the Fokker-Planck operator \mathcal{L} now acting on function $P_s(\mathbf{r}, \mathbf{p})$ defined on the full phase space. The vanishing of $\Delta_{A,B}$ in Eq. (88) simply reflects that trajectories $\mathbf{r}(s), \mathbf{p}(s)$ of length t are as likely as the reversed ones $\mathbf{r}(t-s), -\mathbf{p}(t-s)$ obtained by flipping the momenta.

AOUPs possess an effective equilibrium regime, characterized by a vanishing entropy production rate for small τ , and we thus expect (88) to be valid in such a limit. Let us first show how the computation of $\Delta_{A,B}(t)$ and of the entropy production rate bear some similarities. Using the path-integral methods presented in Sec. IV B, the correlator $\langle \Pi A(t)\Pi B(0) \rangle$ can be

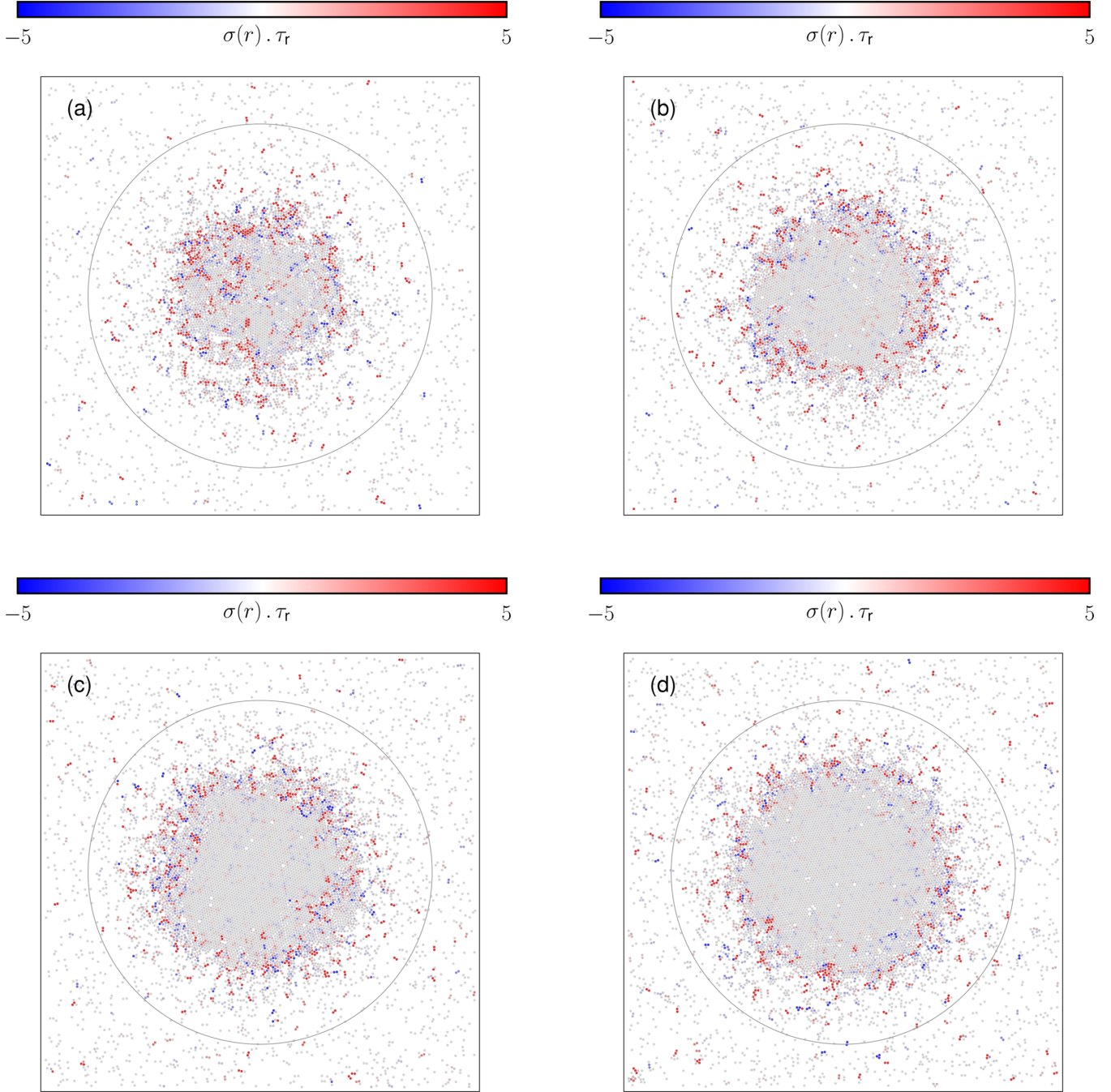


FIG. 6. Snapshots of AOUPs interacting via the short-range soft-core potential (85), and confined in a harmonic potential $U(\mathbf{r}) = U_0(r/a_0)^2$ with finite range a_0 . The range of the potential is represented by the gray circle. The color of each particle refers to the associated instantaneous value of the entropy production rate, expressed in units of $1/\tau_r = \varepsilon/a^2$. We observe that particles form a dense compact cluster centered at the bottom of the harmonic trap with radial symmetry, in contact with a dilute bath of particles. The interface between the dense and dilute phases fluctuates, and the relative size of the dense phase increases with the number of particles from (a) to (d). Number of particles: (a) $N = 5625$, (b) $N = 6750$, (c) $N = 7875$, (d) $N = 9000$. Other parameters: $L = 150$, $D = 1$, $U_0 = 2$, $\varepsilon = 10$, $a = 1$, $\tau = 10$, $a_0 = 60$.

written as

$$\langle \Pi A(t) \Pi B(0) \rangle = \int \mathcal{D}[\mathbf{q}, \mathbf{p}] P_s[\mathbf{q}(0), \mathbf{p}(0)] \delta(\dot{\mathbf{q}} - \mathbf{p}) \times e^{-\mathcal{A}[\mathbf{q}, \mathbf{p}]} \Pi A(t) \Pi B(0), \quad (89)$$

where \mathcal{A} is the dynamical action defined in (74). Changing variable from $(\mathbf{q}(s), \mathbf{p}(s))$ to $(\mathbf{q}^R(s), \mathbf{p}^R(s)) =$

$(\mathbf{q}(t-s), -\mathbf{p}(t-s))$, this can be recast into

$$\langle \Pi A(t) \Pi B(0) \rangle = \int \mathcal{D}[\mathbf{q}^R, \mathbf{p}^R] \delta(\dot{\mathbf{q}}^R - \mathbf{p}^R) P_s[\mathbf{q}^R(t), -\mathbf{p}^R(t)] \times e^{-\mathcal{A}[\mathbf{q}^R, \mathbf{p}^R] + \delta\mathcal{A}[\mathbf{q}^R, \mathbf{p}^R]} A(\mathbf{q}^R(0), \mathbf{p}^R(0)) B(\mathbf{q}^R(t), \mathbf{p}^R(t)), \quad (90)$$

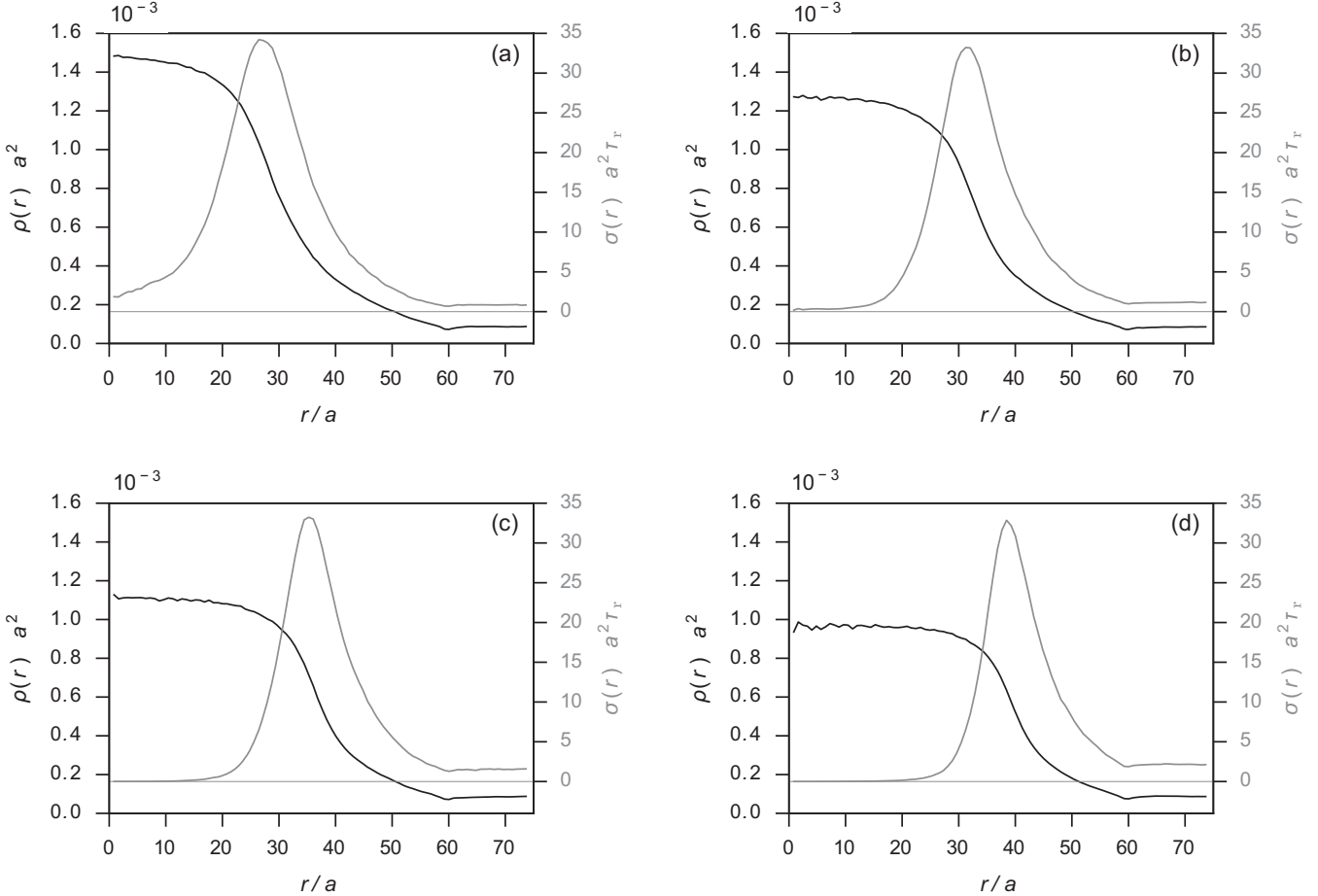


FIG. 7. Density and local entropy production rate profiles as functions of the distance from the center of the harmonic trap. Parameters are the same as in Fig. 6.

where we have used that $\delta\mathcal{A}[\mathbf{q}^R, \mathbf{p}^R] = \mathcal{A}[\mathbf{q}^R, \mathbf{p}^R] - \mathcal{A}[\mathbf{q}, \mathbf{p}]$. Finally, using that

$$P_s[\mathbf{q}^R(t), -\mathbf{p}^R(t)] = P_s[\mathbf{q}^R(0), \mathbf{p}^R(0)] e^{\log \frac{P_s[\mathbf{q}^R(t), -\mathbf{p}^R(t)]}{P_s[\mathbf{q}^R(0), \mathbf{p}^R(0)]}}$$

and dropping the superscript ^R on the dummy variables $\mathbf{q}^R, \mathbf{p}^R$ leads to

$$\Delta_{A,B}(t) = \left\langle A(0)B(t) \left(1 - e^{\delta\mathcal{A}[\mathbf{q}, \mathbf{p}] + \log \frac{P_s[\mathbf{q}(t), -\mathbf{p}(t)]}{P_s[\mathbf{q}(0), \mathbf{p}(0)]}} \right) \right\rangle. \quad (91)$$

The connection to entropy production then comes from the fact that

$$\mathcal{S} = -\lim_{t \rightarrow \infty} \frac{1}{t} \left(\delta\mathcal{A} + \log \frac{P_s[\mathbf{q}(t), -\mathbf{p}(t)]}{P_s[\mathbf{q}(0), \mathbf{p}(0)]} \right). \quad (92)$$

We have shown in Sec. IV B that the entropy production rate scales as $\mathcal{S} \propto \tau^2$ when $\tau \rightarrow 0$. Equation (91) instead involves the total entropy production during a time t . Approximating the latter by $t\mathcal{S}$ would imply that $\Delta_{A,B} \sim (1 - e^{-St}) \rightarrow 0$ as long as $t \ll \tau^{-2}$. This approximation is, however, uncontrolled, and one has to deal, in practice, with the boundary terms that vanish in the computation of \mathcal{S} .

In this section, we thus follow an alternative path, based on an operator formalism, that allows us to treat the small t limit exactly but offers bounds on the decay of $\Delta_{A,B}$ with τ which are weaker than those derived for \mathcal{S} . In the limit

$\tau \rightarrow 0$, the generator of the AOUPs process, i.e., the adjoint of the Fokker-Planck operator, is time-reversal symmetric. As τ increases, it develops a nonsymmetric part, which can be computed using our expansion of the steady-state distribution for small τ . As detailed in Appendix D the leading order of the antisymmetric part of the generator is given by $\tau\mathcal{L}_A^\dagger$, where

$$\mathcal{L}_A^\dagger(\mathbf{q}, \bar{\mathbf{p}}) = \{(\nabla_i \nabla^2 \Phi) - [(\bar{\mathbf{p}}_j \cdot \nabla_j)^2 \nabla_i \Phi]\} \cdot \frac{\partial}{\partial \bar{\mathbf{p}}_i} \quad (93)$$

and we work again with the rescaled variable $\bar{\mathbf{p}} = \sqrt{\tau}\mathbf{p}$. Using perturbation theory [151], we show in Appendix D that

$$\begin{aligned} \Delta_{A,B}(t = \tau u) &= \tau^{3/2} \int_0^u du_1 \int d\mathbf{q} d\bar{\mathbf{p}} P_s(\mathbf{q}, \bar{\mathbf{p}}) A(\mathbf{q}, \bar{\mathbf{p}}) \\ &\times e^{u_1 \sqrt{\tau} \mathcal{L}_A^\dagger(\mathbf{q}, \bar{\mathbf{p}})} \mathcal{L}_A^\dagger(\mathbf{q}, \bar{\mathbf{p}}) e^{(u-u_1)\sqrt{\tau} \mathcal{L}_A^\dagger(\mathbf{q}, \bar{\mathbf{p}})} B(\mathbf{q}, \bar{\mathbf{p}}) \\ &+ O(\tau^2). \end{aligned} \quad (94)$$

Noting that $\sqrt{\tau} \mathcal{L}_A^\dagger \sim O(\tau^0)$, we conclude that, for short times,

$$\Delta_{A,B}(t = \tau u) \sim O(\tau^{3/2}) \quad \text{for} \quad u \sim O(\tau^0). \quad (95)$$

A stronger result than (95) actually holds when at least one of the two observables, say B , depends only on positions: $B = B(\mathbf{q})$. In this case, indeed,

$$\begin{aligned} e^{(u-u_1)\sqrt{\tau} \mathcal{L}_A^\dagger(\mathbf{q}, \bar{\mathbf{p}})} B(\mathbf{q}) &= e^{(u-u_1)\sqrt{\tau} \mathcal{L}_0^\dagger(\mathbf{q}, \bar{\mathbf{p}})} B(\mathbf{q}) + O(\sqrt{\tau}) \\ &= B(\mathbf{q}) + O(\sqrt{\tau}), \end{aligned} \quad (96)$$

where the first equality comes from expanding \mathcal{L} and retaining only its leading order in τ , \mathcal{L}_0 , which is given by

$$\sqrt{\tau}\mathcal{L}_0 \equiv \frac{\partial}{\partial p_{i\alpha}} p_{i\alpha} + D \frac{\partial^2}{\partial p_{i\alpha}^2}. \quad (97)$$

The second equality then follows by noticing that \mathcal{L}_0 acts only on momenta. Inserting (96) in (94) leads to

$$\Delta_{A,B}(t = \tau u) = O(\tau^2), \quad u \sim O(\tau^0). \quad (98)$$

As announced earlier, the effective time-reversal symmetry (TRS) of AOUPs dynamics for small τ thus leads to a corresponding symmetry for two-time correlation functions. The convergence as $\tau \rightarrow 0$ is faster for position-dependent observables than in the full phase space $\mathbf{r}, \bar{\mathbf{p}}$, which is consistent with the fact that momentalike variables have to be handled with care in the context of TRS [45,128,132].

V. EFFECTIVE EQUILIBRIUM: LINEAR RESPONSE AND FLUCTUATION-DISSIPATION RELATIONS

A most celebrated way of probing the nonequilibrium nature of the dynamics lies in investigating the connection between fluctuations and responses. For passive inertial Brownian particles (5), a perturbation of the potential $\Phi \rightarrow \Phi - hB$ amounts to modifying the dynamics into

$$\tau \dot{\mathbf{p}}_i = -\mathbf{p}_i - \nabla_j \Phi + h \nabla_j B + \sqrt{2D} \eta_j. \quad (99)$$

We define the response function R which measures the effect of the perturbation on the average value of an arbitrary observable A as

$$R(t, s) = \left. \frac{\delta \langle A(t) \rangle}{\delta h(s)} \right|_{h=0}. \quad (100)$$

Causality enforces that it vanishes when $t < s$, and time-translation invariance in the steady state means that it only depends on the time difference $t - s$. In equilibrium, fluctuations and response are related by the celebrated fluctuation-dissipation theorem (FDT). The latter states that the response function is related to the decay rate of the (unperturbed) correlations between A and B :

$$R(t, s) = -\frac{1}{D} \frac{d}{dt} \langle A(t) B(s) \rangle. \quad (101)$$

Our aim is to determine to which extent one can obtain a fluctuation-dissipation relation (FDR) analogous to (101) for the active dynamics (1), a topic which has attracted interest recently [152–156]. These works are based on the explicit expression of the steady-state distribution of AOUPs. Here, instead, we follow [41] and proceed at a dynamical level to derive generic relations between response and correlation functions, which do not require any knowledge of the steady state. We then study the response to perturbing the strength of self-propulsion in the effective equilibrium regime.

A. Perturbing with an arbitrary potential

Under the perturbation $\Phi \rightarrow \Phi - hB(\{\mathbf{r}\})$, the dynamics (1) changes as

$$\dot{\mathbf{r}}_i = -\nabla_i \Phi + h \nabla_i B + \mathbf{v}_i. \quad (102)$$

To compute the response function of an observable $A(\{\mathbf{r}\})$, we write the dynamics for $\mathbf{p}_i = \dot{\mathbf{r}}_i$ as

$$\tau \dot{\mathbf{p}}_i = -\mathbf{p}_i - \left(1 + \tau \frac{d}{dt}\right)(\nabla_i \Phi - h \nabla_i B) + \sqrt{2D} \eta_i. \quad (103)$$

Using the formalism of Sec. IV B, the dynamical action becomes

$$\mathcal{A} = \frac{1}{4D} \int_0^t \left| \left(1 + \tau \frac{d}{du}\right)(\mathbf{p}_i + \nabla_i \Phi - h \nabla_i B) \right|^2 du. \quad (104)$$

The probability of a trajectory is given by $\mathcal{P}(\{\mathbf{r}(t), \mathbf{p}(t)\}) \sim \exp[-\mathcal{A}(\{\mathbf{r}(t), \mathbf{p}(t)\})]$, so that $\delta \mathcal{P} = -\delta \mathcal{A} \mathcal{P}$, leading to a response function given by

$$R(t, s) = -\left. \left\langle A(t) \frac{\delta \mathcal{A}}{\delta h(s)} \right\rangle \right|_{h=0}. \quad (105)$$

Note that it is sufficient to compute $\delta \mathcal{A}$ to first order in h :

$$\delta \mathcal{A} = -\frac{1}{2D} \int_0^t h \nabla_i B \cdot \left(1 - \tau^2 \frac{d^2}{du^2}\right)(\mathbf{p}_i + \nabla_i \Phi) du + O(h^2) \quad (106)$$

to determine the response function. We now follow standard procedures [151,157] and we consider the difference $R(t, s) - R(-t, -s)$ in the steady state where time-translation invariance means that $R(t, s) = R(t - s)$. The difference of response functions reads as

$$\begin{aligned} & R(t - s) - R(s - t) \\ &= \frac{1}{2D} \left\langle A(t) \left[\nabla_i B \left(1 - \tau^2 \frac{d^2}{ds^2}\right) (\mathbf{p}_i + \nabla_i \Phi) \right] (s) \right\rangle \\ &\quad - \frac{1}{2D} \left\langle A(-t) \left[\nabla_i B \left(1 - \tau^2 \frac{d^2}{ds^2}\right) (\mathbf{p}_i + \nabla_i \Phi) \right] (-s) \right\rangle. \end{aligned} \quad (107)$$

We now use that, due to time-translation invariance in the steady state, for any two observables A and C we have $\langle A(-t) C(-s) \rangle = \langle A(s) C(t) \rangle$. This leads to

$$\begin{aligned} R(t - s) - R(s - t) &= \frac{1}{2D} \langle A(t) \left[\nabla_i B \left(1 - \tau^2 \frac{d^2}{ds^2}\right) \mathbf{p}_i \right] (s) \rangle \\ &\quad - \frac{1}{2D} \langle A(s) \left[\nabla_i B \left(1 - \tau^2 \frac{d^2}{dt^2}\right) \mathbf{p}_i \right] (t) \rangle \\ &\quad + \frac{1}{2D} \langle A(t) \left[\nabla_i B \left(1 - \tau^2 \frac{d^2}{ds^2}\right) \nabla_i \Phi \right] (s) \rangle \\ &\quad - \frac{1}{2D} \langle A(s) \left[\nabla_i B \left(1 - \tau^2 \frac{d^2}{ds^2}\right) \nabla_i \Phi \right] (t) \rangle. \end{aligned} \quad (108)$$

Using causality, we have that, for $s < t$, $R(s - t) = 0$. Furthermore, in the effective equilibrium regime, the symmetry under a time reversal enforces that the last two lines in (108) cancel out, whereas the first two add up. All in all, the response finally reads as

$$R(t - s) = -\frac{1}{D} \frac{d}{dt} \langle A(t) B(s) \rangle - \frac{\tau^2}{D} \langle A(t) (\ddot{\mathbf{p}}_i \cdot \nabla_i) B(s) \rangle. \quad (109)$$

By contrast to thermal equilibrium, the response is not the time derivative of a given function in general. There are exceptions, for instance, when $B = \sum_i f_i \mathbf{r}_i$, where f_i are a set of constant forces exerted on the particles, as considered in [41].

The two approximate treatments presented previously, based on either UCNA or the Fox theory, lead to Markovian dynamics for the particle positions. Therefore, we can use previous results which predict the form of the response in terms of the stationary distribution [158,159]:

$$R(t, s) = -\frac{d}{dt} \left\langle A(t) \frac{\partial \ln P_S}{\partial h} \Big|_{h=0} (s) \right\rangle, \quad (110)$$

where P_S denotes the stationary distribution under the perturbed potential $\Phi - hB$. From (24), we linearize the distribution around the unperturbed state as

$$\begin{aligned} D \ln P_S = & -\Phi - \frac{\tau}{2} (\nabla_i \Phi)^2 + D \ln |\det \mathbb{M}| \\ & + h(B + \tau \nabla_i \Phi \cdot \nabla_i B - \tau D \nabla_i^2 B) + O(h^2), \end{aligned} \quad (111)$$

yielding

$$R(t) = -\frac{1}{D} \frac{d}{dt} \langle A(t) (B + \tau \nabla_i \Phi \cdot \nabla_i B - \tau D \nabla_i^2 B)(s) \rangle. \quad (112)$$

The result (112), which stems from the Fox theory and UCNA, differs from (109). This shows that UCNA and the Fox theory have to be used with care when studying dynamical observables, even to first order in τ .

B. Perturbing the amplitude of fluctuations

Let us now consider a perturbation $D \rightarrow D[1 + h\Theta(t)]$ in Eq. (2), which can be seen as a change in the typical self-propulsion speed $\sqrt{D/\tau}$ at fixed persistence time. Such perturbation is particularly interesting given the recent experimental development of self-propelled particles, both of synthetic [63,64,160,161] and biological [162–166] natures, whose self-propulsion speed can be controlled by external light sources.

Let us first recall what happens in equilibrium when perturbing the temperature, an operation we denote by $T \rightarrow T[1 + h\Theta(t)]$. Both in the overdamped and in the underdamped cases, the effect of such a perturbation on an arbitrary observable A can be written as [158,167]

$$\langle \delta A(t) \rangle = \frac{h}{T} \langle H(0)[A(0) - A(t)] \rangle, \quad (113)$$

where H is the energy of the system, we set the Boltzmann constant to unity, and $\langle \delta A(t) \rangle = \langle A(t) \rangle_h - \langle A(0) \rangle$. Here, the average $\langle \cdot \rangle_h$ is computed in the presence of the perturbation.

Let us now consider the case of AOUPs. In Appendix E, we show that a similar relation can be derived for times $t \sim \tau$:

$$\langle \delta A(t = s\tau) \rangle = \frac{h}{D} \langle H_{\text{eff}}(0)[A(0) - A(t = s\tau)] \rangle + O(\tau^{3/2}), \quad (114)$$

where

$$\begin{aligned} H_{\text{eff}} &= H_0 + \tau H_1, \\ H_0 &= \Phi + \frac{\bar{\mathbf{p}}_i^2}{2}, \\ H_1 &= \frac{1}{2} [(\nabla_i \Phi)^2 + (\bar{\mathbf{p}}_i \cdot \nabla_i)^2 \Phi - 3D \nabla_i^2 \Phi]. \end{aligned} \quad (115)$$

The above result is the generalization to AOUPs of the equilibrium result (113). Interestingly, H_{eff} is the effective Hamiltonian one would infer from the logarithm of the stationary measure (17) up to order $O(\tau)$. At odds with equilibrium systems where Eq. (113) is valid for all times, Eq. (114) is only derived here for short trajectories.

VI. DYNAMICS OF COLLECTIVE MODES

In this section we study the dynamics of the fluctuating microscopic density and velocity modes. They are defined in terms of the particles' positions and velocities by

$$\rho(\mathbf{r}, t) = \sum_{i=1}^N \delta[\mathbf{r} - \mathbf{r}_i(t)], \quad g_\alpha(\mathbf{r}, t) = \sum_{i=1}^N p_{i\alpha} \delta[\mathbf{r} - \mathbf{r}_i(t)], \quad (116)$$

which are sometimes referred to as empirical measures. Neither ρ nor g_α are hydrodynamic fields in the sense that they are not built from a mesoscopic coarse-graining procedure. They are still fully microscopic (and as such highly singular) objects and one can thus hope to obtain exact evolution equations for them.

For particles evolving according to overdamped Langevin equations, Kawasaki and Dean have shown the steps towards an exact partial differential stochastic equation for the local density field ρ [117,168]. Extracting physical information at hydrodynamic level out of the Dean-Kawasaki equation often requires, however, a further crucial approximation: to replace ρ with a smooth field ρ^H , the hydrodynamic field, and assume that ρ^H still solves the same Dean-Kawasaki equation. Indeed, it is an implicit assumption of most numerical and analytical approaches that one looks only for solutions with sufficient degree of regularity, which ρ^H is assumed to have while ρ clearly has not.

We are aware of only one case where it is possible to prove that the smoothing procedure described above is harmless, in the sense that the evolution of ρ^H obeying the Dean-Kawasaki equation approximates precisely the evolution of ρ . It happens for overdamped particles interacting with a weak potential, that scales as $1/N$. This is a relevant model for either systems with long-range interactions [169] such as interactions mediated by a surrounding low-Reynolds number fluid [170] or for very soft bodies such as polymers [171]. In this case, comparing rigorous mathematical results [172] with those obtained from the Dean-Kawasaki equation allow to conclude that ρ^H captures not only the average evolution of ρ but even its fluctuations up to those whose probability is exponentially small in N [60]. For systems without weak interactions, it remains an outstanding open question the degree of approximation that is involved in passing from the empirical measure ρ to the smooth hydrodynamic field ρ^H .

In the case of systems with underdamped dynamics, a similar procedure to the one leading to the Dean-Kawasaki equation, but now involving both ρ and g_α , was later achieved in [173]. In this case, passing to the hydrodynamic limit would require further assumptions with respect to the case of overdamped particles, even if the equations for ρ and g_α appear to be closed. The main point is that, while some of the steps needed to derive closed equations for ρ and g_α are exactly true when working at the level of the empirical fields ρ and g_α , it is

unclear whether they remain valid in the smoothing required to pass from them to their hydrodynamics counterparts. Taking a different approach, closure at the hydrodynamic level has been discussed by several authors up to very recently [174–179] (see also [115,180] for a more recent discussion within the framework of active matter).

We will not consider the issue due to passing from empirical measures to hydrodynamic fields further in what follows and concentrate instead on deriving the exact equations for ρ and g_α for AOUPs. These could be employed to pass to the hydrodynamic level of description and generate Bogoliubov-Born-Green-Kirkwood-Yvon (BBGKY) type hierarchies or implement approximation methods with no analog within the Lagrangian particle-based formulation, but their development goes beyond the scope of this paper. We limit ourselves, at the end of the section, to sketch future research directions along these lines.

A. Fluctuating hydrodynamics

We first derive the set of equations ruling the coupled dynamics of ρ and \mathbf{g} . The time derivative of the local density of course takes the form of a continuity equation

$$\partial_t \rho(\mathbf{r}, t) = -\partial_\alpha \sum_{i=1}^N \dot{r}_{i\alpha} \delta[\mathbf{r} - \mathbf{r}_i(t)] = -\partial_\alpha g_\alpha(\mathbf{r}, t), \quad (117)$$

thus expressing the conservation of the number of particles. The time derivative of the current density g_α is given by

$$\partial_t g_\alpha(\mathbf{r}, t) = -\partial_\beta \sum_{i=1}^N p_{i\alpha} p_{i\beta} \delta[\mathbf{r} - \mathbf{r}_i(t)] + \sum_{i=1}^N \dot{p}_{i\alpha} \delta[\mathbf{r} - \mathbf{r}_i(t)]. \quad (118)$$

To proceed further, we assume that the particles interact through pairwise interactions only as given in (80). When substituting the microscopic dynamics (4) in the expression for the time derivative of \mathbf{g} , a term of the following form appears:

$$\begin{aligned} & \sum_{i,j=1}^N p_{j\beta} \partial_{i\alpha} \partial_{j\beta} \Phi \delta[\mathbf{r} - \mathbf{r}_i(t)] \\ &= \sum_{i,j,k=1}^N p_{j\beta} \partial_{i\alpha} \partial_{j\beta} V(\mathbf{r}_i - \mathbf{r}_k) \delta[\mathbf{r} - \mathbf{r}_i(t)] \\ &= \sum_{i,k=1}^N (p_{i\beta} \partial_{i\beta} + p_{k\beta} \partial_{k\beta}) \partial_{i\alpha} V(\mathbf{r}_i - \mathbf{r}_k) \delta[\mathbf{r} - \mathbf{r}_i(t)] \\ &= [g_\beta \partial_{\alpha\beta}^2 (V * \rho) - \rho \partial_{\alpha\beta}^2 (V * g_\beta)](\mathbf{r}, t), \end{aligned} \quad (119)$$

where the star $*$ refers to a spatial convolution, e.g. $(V * g_\beta)(\mathbf{x}, t) = \int d\mathbf{y} V(\mathbf{x} - \mathbf{y}) g_\beta(\mathbf{y}, t)$. The dynamic equation for the current density field \mathbf{g} then follows as

$$\begin{aligned} \tau \partial_t g_\alpha + \partial_\beta \kappa_{\alpha\beta} &= -g_\alpha - \tau [g_\beta \partial_{\alpha\beta}^2 (V * \rho) - \rho \partial_{\alpha\beta}^2 (V * g_\beta)] \\ &- \rho \partial_\alpha (V * \rho) + (2D\rho)^{1/2} \Lambda_\alpha. \end{aligned} \quad (120)$$

The noise term Λ_α is Gaussian with correlations

$$\langle \Lambda_\alpha(\mathbf{r}, t) \Lambda_\beta(\mathbf{r}', t') \rangle = \delta_{\alpha\beta} \delta(t - t') \delta(\mathbf{r} - \mathbf{r}'). \quad (121)$$

In Eq. (120) we have introduced a local tensor κ defined by

$$\kappa_{\alpha\beta} = \tau \sum_{i=1}^N p_{i\alpha} p_{i\beta} \delta[\mathbf{r} - \mathbf{r}_i(t)], \quad (122)$$

which can be viewed as the fluctuating analog of the kinetic part of the stress tensor, as described by Irving and Kirkwood in their seminal contribution [see Eq. (5.13) in [108]].

As was noted in [173], with the additional assumption that particles are discernible or that, equivalently for classical particles, there exists a minimal hard-core radius that prevents complete particle overlap unless these are identical, it is possible to rewrite κ in a closed form involving \mathbf{g} and ρ . Indeed, if $\delta(\mathbf{x} - \mathbf{r}_i)\delta(\mathbf{x} - \mathbf{r}_j) = \delta_{ij}\delta(\mathbf{x} - \mathbf{r}_i)\delta(\mathbf{x} - \mathbf{r}_j)$, then

$$\kappa_{\alpha\beta}(\mathbf{r}, t) = \tau \frac{g_\alpha g_\beta}{\rho}. \quad (123)$$

In line with the discussion in the introduction of this section, while the equality in Eq. (123) is obtained working with empirical distributions, it is unclear whether it shall remain valid when passing to the hydrodynamic fields. In any case, the kinetic stress tensor $g_\alpha g_\beta / \rho$ was shown in [173] to be consistent with a kinetic energy $\int d\mathbf{r} \mathbf{g}^2 / (2\rho)$ for equilibrium particles with underdamped dynamics, hence its appeal.

B. A few comments on possible applications

As discussed in [173] for equilibrium underdamped Langevin dynamics, neglecting inertia at the level of the \mathbf{g} field is possible and leads us back to the Dean-Kawasaki equation [117] established directly for equilibrium overdamped Langevin dynamics. An approximation consisting in neglecting some of the inertial contributions for AOUPs is the so-called unified colored-noise one. At the individual particle level, it amounts to formally equating the left-hand side in Eq. (4) to zero. One could then implement the Dean-Kawasaki procedure to arrive at a stochastic partial differential equation for ρ only. The latter would be identical to that obtained by implementing the procedure outlined in Sec. 3.2 of [173] that allows one to evaluate the \mathbf{g} nonlinearity keeping ρ as a slow variable. In a somewhat more controlled fashion, assuming fast equilibration of the \mathbf{g} field in the small τ regime, the latter can be enslaved; this procedure, which basically rests on the replacement $k_{\alpha\beta} \rightarrow \tau D\rho \delta_{\alpha\beta}$, would hold to first order in τ .

It is, however, much more promising to view Eq. (120) [complemented with the continuity equation (117)] as a formal basis to generate approximations for dynamical correlations. To do so, we first rescale the dynamics (120) and (117) to work in the small τ regime. One can then follow the approach developed for equilibrium dynamics in [174,175] to obtain closed equations for two-point correlations. To illustrate the starting point of this procedure, we rescale time and \mathbf{g} just as we did in Sec. II. The resulting equations read as

$$\begin{aligned} \partial_t g_\alpha &= -\gamma \{ g_\alpha + \tau [g_\beta \partial_{\alpha\beta}^2 V * \rho - \rho \partial_{\alpha\beta}^2 (V * g_\beta)] \} \\ &- \rho (\partial_\alpha V * \rho) - \partial_\beta \left(\frac{g_\alpha g_\beta}{\rho} \right) + \sqrt{2D\rho\gamma} \Lambda_\alpha, \end{aligned} \quad (124)$$

where $\gamma = \tau^{-1/2}$, of course supplemented with the local conservation of particles $\partial_t \rho + \nabla \cdot \mathbf{g} = 0$. Written in terms of the local velocity field $\mathbf{u} = \frac{\mathbf{g}}{\rho}$ we have fully equivalently that,

along with $\partial_t \rho = -\nabla \cdot (\rho \mathbf{u})$,

$$\begin{aligned} \partial_t \mathbf{u} + (\mathbf{u} \cdot \nabla) \mathbf{u} &= -\nabla V * \rho - \gamma \mathbf{u} + \sqrt{\frac{2\gamma D}{\rho}} \boldsymbol{\Lambda} \\ &\quad - \gamma \tau \{(\mathbf{u} \cdot \nabla)(\nabla V) * \rho - \rho \nabla \cdot [(\nabla V) * \mathbf{u}]\}. \end{aligned} \quad (125)$$

In an equilibrium framework, the combination $-\gamma \mathbf{g} + \sqrt{2\gamma D\rho} \boldsymbol{\Lambda}$ in Eq. (124) expresses exchanges with a thermostat with an effective friction $\gamma \rho$. The active contribution in Eq. (124), namely $-\gamma \tau [g_\beta \partial_{\alpha\beta}^2 V * \rho - \rho \partial_{\alpha\beta}^2 (V * g_\beta)]$, expresses that friction is enhanced when a minimum of the potential is reached (which effectively pins particles at such a location and which entails added effective attraction). Within a fluctuating hydrodynamics approach, the microscopic friction term $\gamma \rho$ is replaced by a viscosity tensor [174]. We view Eq. (124) as an interesting starting point for controlled coarse-graining procedures which are deferred for future work.

VII. CONCLUSION

Active Ornstein-Uhlenbeck particles were primarily introduced in the field of active matter for the analytical simplification they offer by relaxing the non-normality of the active noise. Since fewer studies exist on AOUPs than on their non-Gaussian counterparts, namely ABPs and RTPs, their phenomenology has been less thoroughly investigated. This article brings our knowledge on AOUPs up to par with that on ABPs and RTPs, as exemplified by Sec. III which report MIPS not only for pairwise forces, but also for a new extension of AOUPs which features quorum-sensing interactions.

Furthermore, a clear gain obtained by working with AOUPs is the possibility to develop a formal small τ approximation of the steady state [41], which is not limited to the first order in τ [37,52–55,61]. As shown in Sec. II, the series can be used to obtain quantitative predictions on

the steady-state distribution, and is not limited to capturing qualitative features, as initially feared by considering only the first order in τ [78].

As shown in Sec. IV, the small τ expansion can be put to work to characterize the departure of AOUPs from their $\tau = 0$ equilibrium limit. In addition, Sec. V shows how linear response can be developed in this nonequilibrium regime, allowing us to predict the response of the system to a perturbation of its self-propulsion as well as to external forcings.

Finally, a natural next stage is to build hydrodynamic descriptions of AOUPs to study both their collective features as well as their transport properties. The technical tools to do so are mature, and presented in Sec. VI. We leave these for future work. For instance, they could potentially help analyze further the dynamical phase transitions reported recently in models of self-propelled particles [134,181–184].

ACKNOWLEDGMENTS

É.F. acknowledges support from an ATTRACT Investigator Grant of the Luxembourg National Research Fund, an Oppenheimer Research Fellowship from the University of Cambridge, and a Junior Research Fellowship from St Catharine's College. C.N. acknowledges the support of Aide Investissements d'Avenir du LabEx PALM (ANR-10-LABX-0039-PALM). J.T. and D.M. acknowledge support from the ANR grant Bactterns. Work funded in part by the European Research Council under the Horizon 2020 Programme, ERC Grant Agreement No. 740269. M.E.C. is funded by the Royal Society.

APPENDIX A: STATIONARY MEASURE FOR ONE PARTICLE IN A ONE-DIMENSIONAL DOMAIN

At order τ^2 , the exact one-dimensional stationary measure takes the form

$$\begin{aligned} P_s(r, p) = e^{-\frac{\phi}{D} - \frac{p^2}{2D}} &\left[c + \tau \left(\frac{3c\phi^{(2)}}{2} - \frac{c\phi^{(1)2}}{2D} - c \frac{p^2\phi^{(2)}}{2D} + c_1 \right) + \tau^{\frac{3}{2}} \left(-\frac{1}{2}cp\phi^{(3)} + \frac{cp^3\phi^{(3)}}{6D} \right) \right. \\ &+ \tau^2 \left(-p^4 \frac{c\phi^{(4)}}{24D} + p^4 \frac{c\phi^{(2)2}}{8D^2} + p^2 \frac{c\phi^{(1)}\phi^{(3)}}{4D} + p^2 \frac{c\phi^{(1)2}\phi^{(2)}}{4D^2} - p^2 \frac{3c\phi^{(2)2}}{4D} - p^2 \frac{c_1\phi^{(2)}}{2D} + a_2 \int^r e^{\frac{\phi}{D}} dx \right. \\ &- \frac{c_1\phi^{(1)2}}{2D} + \frac{c \int \phi^{(1)2}\phi^{(3)}dx}{2D} + c_2 + \frac{c\phi^{(1)4}}{8D^2} + \frac{3c_1\phi^{(2)}}{2} + \frac{5c\phi^{(2)2}}{8} - \frac{5c\phi^{(1)}\phi^{(3)}}{4} + \frac{5Dc\phi^{(4)}}{8} \Big) \\ &+ \tau^{\frac{5}{2}} \left(-a_2 e^{\frac{\phi}{D}} p - p \frac{c_1\phi^{(3)}}{2} + p \frac{c\phi^{(1)2}\phi^{(3)}}{4D} + p \frac{c\phi^{(2)}\phi^{(3)}}{2} + p \frac{5c\phi^{(1)}\phi^{(4)}}{12} - p \frac{7Dc\phi^{(5)}}{24} + p^3 \frac{c_1\phi^{(3)}}{6D} - p^3 \frac{c\phi^{(1)2}\phi^{(3)}}{12D^2} \right. \\ &\left. \left. + p^3 \frac{c\phi^{(2)}\phi^{(3)}}{4D} - p^3 \frac{5c\phi^{(1)}\phi^{(4)}}{36D} + p^5 \frac{c\phi^{(5)}}{120D} - p^5 \frac{c\phi^{(3)}\phi^{(2)}}{12D^2} \right) \right], \end{aligned}$$

where explicit dependencies on r and p have been omitted when unambiguous and c, c_1, c_2, a_2 are integration constants. We can thus compute the constant steady-state current

$$J = -\sqrt{2\pi} a_2 D^2 \tau^2 + o(\tau^2). \quad (A1)$$

Integrating over the p variable, we then obtain

$$\begin{aligned} P_s(r) = \sqrt{2\pi D^2} e^{-\frac{\phi}{D}} &\left[(c + \tau c_1) + \tau \left(c\phi^{(2)} - c \frac{\phi^{(1)2}}{2D} \right) \right. \\ &+ \tau^2 \left(\frac{cD\phi^{(4)}}{2} + \frac{c\phi^{(2)2}}{4} - c\phi^{(1)}\phi^{(3)} \right) \end{aligned}$$

$$+ c \frac{\int \phi^{(1)} \phi^{(3)} dx}{2D} + c \frac{\phi^{(1)} \phi^{(2)}}{4D} + c_1 \phi^{(2)} \\ + a_2 \int e^{\frac{\phi}{D}} dx \Big]. \quad (\text{A2})$$

The integration constants then depend on the choice of boundary conditions. First, we consider the case of a particle in an infinite domain and thus require the potential to be confining. In this case, the term $e^{-\frac{\phi(r)}{D}} a_2 \int_0^r e^{\frac{\phi}{D}} dx$ does not vanish automatically in the limit $r \rightarrow \pm\infty$ and a_2 thus has to vanish. As expected, this leads to a vanishing current J . The constants c_i are then set by normalization at each order

$$P_S(r) \sim \exp \left[-\frac{\Phi}{D} + \tau \left(\Phi''(r) - \frac{\Phi'(r)^2}{2D} \right) + \tau^2 \left(\frac{D\Phi^{(4)}(r)}{2} + \frac{\int_0^r \Phi'(y)^2 \Phi^{(3)}(y) dy}{2D} - \Phi'(r)\Phi^{(3)}(r) - \frac{\Phi''(r)^2}{4} \right. \right. \\ \left. \left. - \frac{\Phi'(r)^4}{8D^2} + \frac{3\Phi'(r)^2 \Phi''(r)}{4D} - \frac{\int_0^r e^{\frac{\phi}{D}} \int_0^L \Phi'^2 \Phi^{(3)} dr}{2D \int_0^L e^{\frac{\phi}{D}}} + \frac{\Phi'(r)^2 \int_0^L e^{-\frac{\phi}{D}} (\frac{\Phi'^2}{2D} - \Phi^{(2)})}{2D \int_0^L e^{-\frac{\phi}{D}}} \right) + O(\tau^3) \right].$$

The last lines differs from the case of a confining potential; it enforces periodic boundary conditions and leads to the nonvanishing current (72).

APPENDIX B: APPROXIMATE DYNAMICS

We present in this Appendix two approximate forms of the dynamics of interacting persistent self-propelled particles. They are inspired by approximation schemes which were originally proposed for noninteracting particles: the unified colored-noise approximation [54,55] and the Fox theory [52,53].

We derive the stationary distribution of the unified colored-noise approximation (UCNA). To this aim, we turn the multiplicative Langevin equation, written with the Stratonovich convention in (22), into an additive one by introducing the following change of variables:

$$q_{i\alpha} = \int \mathbb{M}_{i\alpha, j\beta} dr_{j\beta}, \quad (\text{B1})$$

so that the Jacobian between \mathbf{q}_i and \mathbf{r}_i is given by $|\det \mathbb{M}|$. The corresponding Langevin equation reads as

$$\dot{q}_{i\alpha} = -\frac{\partial \Phi}{\partial r_{i\alpha}} - (2D)^{1/2} \eta_{i\alpha}. \quad (\text{B2})$$

One can explicitly check that this is an equilibrium Langevin dynamics for \mathbf{q} because

$$\frac{\partial \Phi}{\partial r_{i\alpha}} = \frac{\partial [\Phi + \frac{\tau}{2} (\nabla_{\mathbf{r}} \Phi)^2]}{\partial q_{i\alpha}} \quad (\text{B3})$$

which means that the force in \mathbf{q} space, and thus in \mathbf{r} space, is conservative. It is then straightforward to write the corresponding Fokker-Planck equation, from which we deduce the stationary distribution as

$$P_S(\{\mathbf{q}_i\}) \sim \exp \left(-\frac{1}{D} \int \frac{\partial \Phi}{\partial r_{i\alpha}} dq_{i\alpha} \right), \quad (\text{B4})$$

τ^i . The expression (20) in the main text then comes from exponentiating Eq. (A2).

Second, in the case of a periodic potential with finite support, a_2 must instead be set by requiring the periodicity of the steady-state distribution (A2). For a system of size L , this gives

$$a_2 = -\frac{c \int_0^L \phi^{(1)} \phi^{(3)} dx}{2D \int_0^L e^{\frac{\phi}{D}} dx}. \quad (\text{A3})$$

Altogether, we arrive at

leading to

$$P_S(\{\mathbf{r}_i\}) \sim \exp \left(-\frac{1}{D} \int \frac{\partial \Phi}{\partial r_{i\alpha}} \mathbb{M}_{i\alpha, j\beta} dr_{j\beta} \right) |\det \mathbb{M}|. \quad (\text{B5})$$

Using $\mathbb{M}_{i\alpha, j\beta} = \delta_{ij} \delta_{\alpha\beta} + \tau \partial_{i\alpha}^2 \Phi$, the explicit expression of the stationary distribution (24) follows directly. Note that the above derivation shows that UCNA does not solely provide an effective potential for the dynamics: it is a purely equilibrium approximation of the latter, and hence it is unable to capture nonequilibrium features such as the emergence of currents in ratchet potentials as discussed in Sec. IV A.

Another approximate dynamics can be derived by using functional calculus on the weight \mathcal{P} of a given time realization of the noises. Introducing the kernel \mathcal{K} defined in terms of the self-propulsion correlations as

$$\int \mathcal{K}(t-u) \langle v_{i\alpha}(s) v_{j\beta}(u) \rangle du = \delta(t-s) \delta_{ij} \delta_{\alpha\beta}, \quad (\text{B6})$$

we write the probability weight \mathcal{P} as

$$\mathcal{P} = \exp \left[-\frac{1}{2} \iint_0^t \mathcal{K}(u-s) v_{i\alpha}(u) v_{i\alpha}(s) du ds \right]. \quad (\text{B7})$$

The distribution of positions at a given time t can be expressed in terms of this probability weight as

$$P(\{\mathbf{r}_i\}, t) = \int \mathcal{P} \prod_{k=1}^N \delta[\mathbf{r}_k - \mathbf{q}_k(t)] \mathcal{D}\mathbf{v}_k, \quad (\text{B8})$$

where the positions \mathbf{q}_k satisfy the dynamics $\dot{\mathbf{q}}_k = -\nabla_k \Phi + \mathbf{v}_k$. It follows that the time derivative of this distribution reads as

$$\begin{aligned} \partial_t P &= \nabla_i \cdot \left\{ \int \mathcal{P} [\nabla_i \Phi - \mathbf{v}_i] \prod_{k=1}^N \delta[\mathbf{r}_k - \mathbf{q}_k(t)] \mathcal{D}\mathbf{v}_k \right\} \\ &= -\nabla_i \cdot \left\{ \int \mathcal{P} \mathbf{v}_i(t) \prod_{k=1}^N \delta[\mathbf{r}_k - \mathbf{q}_k(t)] \mathcal{D}\mathbf{v}_k \right\} \\ &\quad + \nabla_i \cdot (P \nabla_i \Phi). \end{aligned} \quad (\text{B9})$$

To proceed further, we note that

$$\begin{aligned} v_{i\alpha}(t)\mathcal{P} &= \mathcal{P} \int \delta(t-s)v_{i\alpha}(s)ds \\ &= - \int_0^\infty \langle v_{l\gamma}(t)v_{l\gamma}(s) \rangle \frac{\delta\mathcal{P}}{\delta v_{i\alpha}(s)} ds, \end{aligned} \quad (\text{B10})$$

where we have used Eqs. (B6) and (B7). It leads to

$$\begin{aligned} &\int \mathcal{P}v_{i\alpha} \prod_{k=1}^N \delta[\mathbf{r}_k - \mathbf{q}_k(t)]\mathcal{D}\mathbf{v}_k \\ &= - \int_0^\infty \langle v_{l\gamma}(s)v_{l\gamma}(t) \rangle ds \int \frac{\delta\mathcal{P}}{\delta v_{i\alpha}(s)} \\ &\quad \times \prod_{k=1}^N \delta[\mathbf{r}_k - \mathbf{q}_k(t)]\mathcal{D}\mathbf{v}_k \\ &= -\nabla_j \cdot \int_0^\infty \langle v_{l\gamma}(s)v_{l\gamma}(t) \rangle ds \int \mathcal{P} \frac{\delta\mathbf{q}_j(t)}{\delta v_{i\alpha}(s)} \\ &\quad \times \prod_{k=1}^N \delta[\mathbf{r}_k - \mathbf{q}_k(t)]\mathcal{D}\mathbf{v}_k, \end{aligned} \quad (\text{B11})$$

where we have integrated by parts with respect to $v_{i\alpha}$ to get the second line. From the dynamics $\dot{\mathbf{q}}_i = -\nabla_i\Phi + \mathbf{v}_i$, we obtain the following identity:

$$\frac{d}{dt} \frac{\delta q_{j\beta}(t)}{\delta v_{i\alpha}(s)} = -\frac{\delta q_{j\beta}(t)}{\delta v_{i\alpha}(s)} \frac{\partial^2 \Phi}{\partial q_{i\alpha} \partial q_{j\beta}} + \delta_{ij} \delta_{\alpha\beta} \delta(t-s). \quad (\text{B12})$$

This equation contains a sum which was omitted in [40]. Introducing the Hessian \mathbb{H} with elements $\mathbb{H}_{i\alpha,j\beta} = \partial^2 \Phi / (\partial q_{i\alpha} \partial q_{j\beta})$, the solution can be written for $t > s$ as

$$\frac{\delta q_{j\beta}(t)}{\delta v_{i\alpha}(s)} = [e^{-\int_s^t \mathbb{H}(w)dw}]_{i\alpha,j\beta}. \quad (\text{B13})$$

Substituting in Eq. (B11) and using $\langle v_{l\gamma}(t)v_{l\gamma}(s) \rangle = De^{-|t-s|/\tau}$, we get

$$\begin{aligned} &\int \mathcal{P}v_{i\alpha} \prod_{k=1}^N \delta[\mathbf{r}_k - \mathbf{q}_k(t)]\mathcal{D}\mathbf{v}_k \\ &= \frac{D}{\tau} \partial_{j\beta} \left\{ \int \mathcal{P} \int_0^t e^{-(t-s)/\tau} [e^{-\int_s^t \mathbb{H}(w)dw}]_{i\alpha,j\beta} ds \right. \\ &\quad \left. \prod_{k=1}^N \delta[\mathbf{r}_k - \mathbf{q}_k(t)]\mathcal{D}\mathbf{v}_k \right\} \\ &= D\partial_{j\beta}(P\mathbb{D}_{i\alpha,j\beta}), \end{aligned} \quad (\text{B14})$$

where we have introduced the diffusion tensor \mathbb{D} as

$$\begin{aligned} \mathbb{D}(t) &= \int_0^t e^{-(t-s)/\tau} e^{-\int_s^t \mathbb{H}(w)dw} ds \\ &= \int_0^t e^{-u/\tau} e^{-\int_{t-u}^t \mathbb{H}(w)dw} du. \end{aligned} \quad (\text{B15})$$

This is valid for any value of τ since we have not used any approximation at this stage of the derivation. To get rid of the kernel in \mathbb{D} , we assume that \mathbb{H} varies slowly in time, in the

same spirit as the original Fox theory [52,53]:

$$\int_{t-u}^t \mathbb{H}(w)dw \simeq u\mathbb{H}(t), \quad (\text{B16})$$

yielding

$$\mathbb{D}(t) \simeq \int_0^t e^{-u/\tau} e^{-u\mathbb{H}(t)} du = \int_0^t e^{-u\mathbb{M}(t)/\tau} du, \quad (\text{B17})$$

where we have used $\mathbb{M}_{i\alpha,j\beta} = \delta_{ij} \delta_{\alpha\beta} + \tau \mathbb{H}_{i\alpha,j\beta}$. Integrating and performing the same approximation as Fox gives

$$\mathbb{D}(t) \simeq \tau \mathbb{M}^{-1}(t)[1 - e^{-t\mathbb{M}(t)/\tau}] \simeq \tau \mathbb{M}^{-1}(t). \quad (\text{B18})$$

The Fokker-Planck equation (25) follows directly.

APPENDIX C: TIME REVERSAL, TIME-TRANSLATIONAL INVARIANCE, AND TIME-REVERSED PROCESS

To discuss time-reversal symmetry, we introduce the Markov process that corresponds to the time-reversed process of the original one. The latter is defined as follows: it is the Markov process that generates a time-reversed trajectory $\mathbf{r}(t_f - t), -\mathbf{p}(t_f - t)$ with the same probability as the original process generates the original trajectory $\mathbf{r}(t), \mathbf{p}(t)$, where t_f is the length of the trajectory. We denote \mathcal{L}^\dagger and \mathcal{L}_r^\dagger the generators of the original Markov process and of its time-reversed counterpart, respectively. Note that the reversed process is not obtained by simply reversing time in the original dynamics; the dynamics obtained in this way would not satisfy the Markov property. This is well known in the mathematical literature; the reversed process was rigorously constructed by Haussmann and Padoux in [185] (see [186] for a detailed presentation).

Introducing the operator $\Pi f(\mathbf{q}, \mathbf{p}) = f(\mathbf{q}, -\mathbf{p})$, time-translation invariance imposes that

$$\langle B(t)A(0) \rangle = \langle B(0)A(-t) \rangle = \langle \Pi B(0)\Pi A(t) \rangle_r, \quad (\text{C1})$$

where the last equality can be regarded as a mathematical definition of the reversed process. The last average in (C1) is then defined as

$$\begin{aligned} &\langle \Pi B(0)\Pi A(t) \rangle_r \\ &\equiv \int d\mathbf{q} d\mathbf{p} P_s^R(\mathbf{q}, \mathbf{p}) B(\mathbf{q}, -\mathbf{p}) e^{t\mathcal{L}_r^\dagger(\mathbf{q}, \mathbf{p})} A(\mathbf{q}, -\mathbf{p}), \end{aligned} \quad (\text{C2})$$

where P_s^R is the stationary distribution of the time-reversed process, which satisfies $P_s^R(\mathbf{q}, \mathbf{p}) = \Pi P_s(\mathbf{q}, \mathbf{p})$. From Eq. (C1) we thus have

$$\begin{aligned} &\int d\mathbf{q} d\mathbf{p} P_s(\mathbf{q}, \mathbf{p}) A(\mathbf{q}, \mathbf{p}) (e^{t\mathcal{L}^\dagger(\mathbf{q}, \mathbf{p})} B)(\mathbf{q}, \mathbf{p}) \\ &= \int d\mathbf{q} d\mathbf{p} (\Pi P_s)(\mathbf{q}, \mathbf{p}) (\Pi B)(\mathbf{q}, \mathbf{p}) e^{t\mathcal{L}_r^\dagger(\mathbf{q}, \mathbf{p})} (\Pi A)(\mathbf{q}, \mathbf{p}). \end{aligned} \quad (\text{C3})$$

This equality holds for any time t and observables A, B . Taking its time derivative and setting $t = 0$ leads, after integrating by parts, to

$$\mathcal{L}_r^\dagger = \Pi P_s^{-1} \mathcal{L} P_s \Pi. \quad (\text{C4})$$

Note that Eq. (C4) also implies that

$$e^{t\mathcal{L}_r^\dagger} = \Pi P_s^{-1} e^{t\mathcal{L}} P_s \Pi. \quad (\text{C5})$$

A check that \mathcal{L}_r^\dagger defined as (C4) indeed satisfies Eq. (C1) then stems from rewriting the right-hand side of Eq. (C2) as

$$\begin{aligned} \langle \Pi B(0) \Pi A(t) \rangle_r &= \int d\mathbf{q} d\mathbf{p} [\Pi P_s(\mathbf{q}, \mathbf{p}) \Pi B(\mathbf{q}, \mathbf{p})] \\ &\times \Pi P_s^{-1} e^{\tau \mathcal{L}} P_s \Pi \Pi A(\mathbf{q}, \mathbf{p}), \end{aligned} \quad (\text{C6})$$

which leads to

$$\langle \Pi B(0) \Pi A(t) \rangle_r = \int d\mathbf{q} d\mathbf{p} B(\mathbf{q}, \mathbf{p}) e^{\tau \mathcal{L}} P_s A(\mathbf{q}, \mathbf{p}) \quad (\text{C7})$$

or, equivalently, to

$$\langle \Pi B(0) \Pi A(t) \rangle_r = \langle B(t) A(0) \rangle. \quad (\text{C8})$$

The definition of time-reversal symmetry is that $\mathcal{L}_r = \mathcal{L}$. One then has that $P_s^R = P_s$. The left-hand side of (C8) can then be written as $\langle \Pi B(0) \Pi A(t) \rangle_r = \langle \Pi B(0) \Pi A(t) \rangle$ so that we finally have

$$\langle \Pi B(0) \Pi A(t) \rangle = \langle B(t) A(0) \rangle \quad (\text{C9})$$

which is Eq. (88) of the main text.

APPENDIX D: SYMMETRY OF TIME CORRELATIONS

We present a derivation of the asymmetry of time correlations, quantified by Δ_{AB} in (95) and (94), using the reverse process introduced in Appendix C. When detailed balance holds, $\mathcal{L}_r^\dagger = \mathcal{L}^\dagger$ so that the reverse process is the original dynamics, as expected since equilibrium dynamics is invariant under time reversal in the steady state. For AOUPs, using the approximate stationary measure (17) and the definition of \mathcal{L}_r^\dagger in Eq. (C4), we obtain

$$\mathcal{L}_r^\dagger(\mathbf{r}, \bar{\mathbf{p}}) = \mathcal{L}^\dagger(\mathbf{r}, \bar{\mathbf{p}}) + \tau \mathcal{L}_A^\dagger(\mathbf{r}, \bar{\mathbf{p}}) + O(\tau^{3/2}), \quad (\text{D1})$$

where $\bar{\mathbf{p}} = \sqrt{\tau} \mathbf{p}$ has been introduced in the main text and the leading-order antisymmetric part is given by

$$\mathcal{L}_A^\dagger(\mathbf{r}, \bar{\mathbf{p}}) = \{(\nabla_i \nabla^2 \Phi) - [(\bar{\mathbf{p}}_j \cdot \nabla_j)^2 \nabla_i \Phi]\} \cdot \frac{\partial}{\partial \bar{\mathbf{p}}_i}. \quad (\text{D2})$$

We thus see that detailed balance holds perturbatively in τ in the full $(\mathbf{r}, \bar{\mathbf{p}})$ space, though it only holds up to order $\sqrt{\tau}$ when $\bar{\mathbf{p}}$ is not integrated out.

We now want to show that the asymmetry of time correlations Δ_{AB} satisfies the expansion (94). By definition, we have

$$\langle \Pi A(t) \Pi B(0) \rangle = \int d\bar{\mathbf{p}} d\mathbf{q} P_s(\mathbf{q}, \bar{\mathbf{p}}) (\Pi B)(\mathbf{q}, \bar{\mathbf{p}}) e^{\tau \mathcal{L}^\dagger} \Pi A(\mathbf{q}, \bar{\mathbf{p}}). \quad (\text{D3})$$

Taking the adjoint of Eq. (C5) and reorganizing the integral leads to

$$\langle \Pi A(t) \Pi B(0) \rangle = \int d\bar{\mathbf{p}} d\mathbf{q} (\Pi P_s)(\mathbf{q}, \bar{\mathbf{p}}) A(\mathbf{q}, \bar{\mathbf{p}}) e^{\tau \mathcal{L}_r^\dagger} B(\mathbf{q}, \bar{\mathbf{p}}). \quad (\text{D4})$$

Using the rescaled time $t = \sqrt{\tau} \bar{t}$, we can thus rewrite $\Delta_{AB}(\bar{t})$ as

$$\begin{aligned} \Delta_{AB}(\bar{t}) &= \int d\mathbf{q} d\bar{\mathbf{p}} P_s(\mathbf{q}, \bar{\mathbf{p}}) A(\mathbf{q}, \bar{\mathbf{p}}) \\ &\times \left(e^{\bar{t} \mathcal{L}^\dagger(\mathbf{q}, \bar{\mathbf{p}})} - \frac{P_s(\mathbf{q}, -\bar{\mathbf{p}})}{P_s(\mathbf{q}, \bar{\mathbf{p}})} e^{\bar{t} \mathcal{L}_r^\dagger(\mathbf{q}, \bar{\mathbf{p}})} \right) B(\mathbf{q}, \bar{\mathbf{p}}). \end{aligned} \quad (\text{D5})$$

Note that, for Kramers dynamics [187], $\mathcal{L}_r^\dagger = \mathcal{L}^\dagger$ and $P_s(\mathbf{q}, -\bar{\mathbf{p}}) = P_s(\mathbf{q}, \bar{\mathbf{p}})$ implies that $\Delta_{A,B}(\bar{t}) = 0$, as expected. For AOUPs, using the stationary measure (17) to expand $P_s(\mathbf{q}, -\bar{\mathbf{p}})/P_s(\mathbf{q}, \bar{\mathbf{p}})$ for small τ , we find

$$\begin{aligned} \Delta_{A,B}(\bar{t}) &= \int d\mathbf{q} d\bar{\mathbf{p}} P_s(\mathbf{q}, \bar{\mathbf{p}}) A(\mathbf{q}, \bar{\mathbf{p}}) \\ &\times (e^{\bar{t} \mathcal{L}^\dagger(\mathbf{q}, \bar{\mathbf{p}})} - e^{\bar{t} \mathcal{L}_r^\dagger(\mathbf{q}, \bar{\mathbf{p}})}) B(\mathbf{q}, \bar{\mathbf{p}}) + O(\tau^{3/2}). \end{aligned} \quad (\text{D6})$$

Using linear response [167], we note that the difference between the two evolution operators can be evaluated as

$$\begin{aligned} &[e^{\bar{t} \mathcal{L}^\dagger(\mathbf{q}, \bar{\mathbf{p}})} - e^{\bar{t} \mathcal{L}_r^\dagger(\mathbf{q}, \bar{\mathbf{p}})}] \\ &= \tau \int_0^{\bar{t}} ds_1 e^{s_1 \mathcal{L}^\dagger(\mathbf{q}, \bar{\mathbf{p}})} \mathcal{L}_A^\dagger(\mathbf{q}, \bar{\mathbf{p}}) e^{(\bar{t}-s_1) \mathcal{L}^\dagger(\mathbf{q}, \bar{\mathbf{p}})} + O(\tau^2), \end{aligned} \quad (\text{D7})$$

where $\mathcal{L}_A^\dagger(\mathbf{q}, \bar{\mathbf{p}})$ is the leading order antisymmetric part of the generator of AOUPs dynamics, given in (D2). Plugging (D7) in (D6) we obtain

$$\begin{aligned} \Delta_{A,B}(\bar{t}) &= \tau \int_0^{\bar{t}} ds_1 \int d\mathbf{q} d\bar{\mathbf{p}} P_s(\mathbf{q}, \bar{\mathbf{p}}) A(\mathbf{q}, \bar{\mathbf{p}}) \\ &\times e^{s_1 \mathcal{L}^\dagger(\mathbf{q}, \bar{\mathbf{p}})} \mathcal{L}_A^\dagger(\mathbf{q}, \bar{\mathbf{p}}) e^{(\bar{t}-s_1) \mathcal{L}^\dagger(\mathbf{q}, \bar{\mathbf{p}})} B(\mathbf{q}, \bar{\mathbf{p}}) + O(\tau^{3/2}). \end{aligned} \quad (\text{D8})$$

Finally, using the explicit expression of \mathcal{L}_A^\dagger and rescaling time as $s_1 = u_1 \sqrt{\tau}$, we obtain Eq. (94), which was the goal of this Appendix.

APPENDIX E: PERTURBATION OF THE SELF-PROPELLION SPEED

We present in this Appendix a derivation of Eq. (114). To do so, we apply the Agarwal formula [151,158] which states that the response of an observable A to the perturbation $D \rightarrow D[1 + h\Theta(t)]$ is given by

$$\langle \delta A(\bar{t}) \rangle = \int_0^{\bar{t}} ds \left\langle \frac{\mathcal{L}_p P_s}{P_s}(0) A(s) \right\rangle + O(h^2), \quad (\text{E1})$$

where \mathcal{L}_p is the Fokker-Planck operator corresponding to the perturbation

$$\mathcal{L}_p(\bar{\mathbf{p}}) = \frac{hD}{\sqrt{\tau}} \frac{\partial^2}{\partial \bar{\mathbf{p}}_i^2}. \quad (\text{E2})$$

In order to obtain Eq. (114) from (E1), we first note that, inserting expression (17) for P_s into (E1) leads to

$$\frac{1}{h} \frac{\mathcal{L}_p(\bar{\mathbf{p}}) P_s(\mathbf{q}, \bar{\mathbf{p}})}{P_s(\mathbf{q}, \bar{\mathbf{p}})} = -\frac{1}{D} \mathcal{L}_r^\dagger(\mathbf{q}, -\bar{\mathbf{p}}) H_{\text{eff}}(\mathbf{q}, \bar{\mathbf{p}}) + O(\tau), \quad (\text{E3})$$

where H_{eff} is defined as

$$\begin{aligned} H_{\text{eff}} &= H_0 + \tau H_1, \\ H_0 &= \Phi + \frac{\bar{\mathbf{p}}_i^2}{2}, \\ H_1 &= \frac{1}{2} [(\nabla_i \Phi)^2 + (\bar{\mathbf{p}}_i \cdot \nabla_i)^2 \Phi - 3D \nabla_i^2 \Phi]. \end{aligned} \quad (\text{E4})$$

Equation (E1) can thus be rewritten as

$$\langle \delta A(\bar{t}) \rangle = -\frac{\hbar}{D} \int_0^{\bar{t}} ds \langle (\Pi \mathcal{L}_r^\dagger) H_{\text{eff}}(0) A(s) \rangle + O(\tau, h^2). \quad (\text{E5})$$

Then, from the definition of time-translational invariance, we have that

$$\begin{aligned} & \int d\mathbf{q} d\mathbf{p} P_s(\mathbf{q}, \mathbf{p}) H_{\text{eff}}(\mathbf{q}, \mathbf{p}) (e^{s\mathcal{L}_r^\dagger(\mathbf{q}, \mathbf{p})} A)(\mathbf{q}, \mathbf{p}) \\ &= \int d\mathbf{q} d\mathbf{p} (\Pi P_s)(\mathbf{q}, \mathbf{p}) (\Pi A)(\mathbf{q}, \mathbf{p}) e^{s\mathcal{L}_r^\dagger(\mathbf{q}, \mathbf{p})} (\Pi H_{\text{eff}})(\mathbf{q}, \mathbf{p}). \end{aligned} \quad (\text{E6})$$

Taking the time derivative of this equality at time $s = 0$ and using Eq. (C5) then leads to

$$\langle H(0) L^\dagger A(s) \rangle = \langle A(s) (\Pi L_r^\dagger) H_{\text{eff}}(0) \rangle. \quad (\text{E7})$$

Using that $\partial_s A(s) = L^\dagger A(s)$, Eq. (E5) can thus be finally rewritten as

$$\langle \delta A(\bar{t}) \rangle = -\frac{\hbar}{D} \int_0^{\bar{t}} ds \left\langle H_{\text{eff}}(0) \frac{dA(s)}{ds} \right\rangle + O(\tau, h^2). \quad (\text{E8})$$

Then, using $\bar{t} = s\sqrt{\tau}$ with $s \sim O(\tau^0)$ and integrating, we obtain Eq. (114).

Note that, again, we did not use the path-integral techniques described in Sec. V A for describing perturbations obtained by applying an external force. The operatorial approach we followed here holds for short trajectories, albeit we expect the result to be valid for longer ones. An interesting alternative approach would be to generalize the analysis presented in [188,189] which uses path-integral formulation to solve a similar problem, albeit in equilibrium.

-
- [1] T. B. Saw, A. Doostmohammadi, V. Nier, L. Kocgozlu, S. Thampi, Y. Toyama, P. Marcq, C. T. Lim, J. M. Yeomans, and B. Ladoux, *Nature (London)* **544**, 212 (2017).
- [2] K. Kawaguchi, R. Kageyama, and M. Sano, *Nature (London)* **545**, 327 (2017).
- [3] M. Guo, A. J. Ehrlicher, M. H. Jensen, M. Renz, J. R. Moore, R. D. Goldman, J. Lippincott-Schwartz, F. C. Mackintosh, and D. A. Weitz, *Cell* **158**, 822 (2014).
- [4] W. W. Ahmed, É. Fodor, M. Almonacid, M. Bussonnier, M.-H. Verlhac, N. Gov, P. Visco, F. van Wijland, and T. Betz, *Biophys. J.* **114**, 1667 (2018).
- [5] J. R. Howse, R. A. L. Jones, A. J. Ryan, T. Gough, R. Vafabakhsh, and R. Golestanian, *Phys. Rev. Lett.* **99**, 048102 (2007).
- [6] J. Palacci, C. Cottin-Bizonne, C. Ybert, and L. Bocquet, *Phys. Rev. Lett.* **105**, 088304 (2010).
- [7] G. Volpe, I. Buttinoni, D. Vogt, H.-J. Küpperer, and C. Bechinger, *Soft Matter* **7**, 8810 (2011).
- [8] A. Bricard, J.-B. Caussin, N. Desreumaux, O. Dauchot, and D. Bartolo, *Nature (London)* **503**, 95 (2013).
- [9] D. Nishiguchi and M. Sano, *Phys. Rev. E* **92**, 052309 (2015).
- [10] M. N. van der Linden, L. C. Alexander, D. G. A. L. Aarts, and O. Dauchot, *Phys. Rev. Lett.* **123**, 098001 (2019).
- [11] J. Yan, M. Han, J. Zhang, C. Xu, E. Luijten, and S. Granick, *Nat. Mater.* **15**, 1095 (2016).
- [12] D. Volfson, A. Kudrolli, and L. S. Tsimring, *Phys. Rev. E* **70**, 051312 (2004).
- [13] V. Narayan, S. Ramaswamy, and N. Menon, *Science* **317**, 105 (2007).
- [14] J. Deseigne, O. Dauchot, and H. Chaté, *Phys. Rev. Lett.* **105**, 098001 (2010).
- [15] J. Toner and Y. Tu, *Phys. Rev. Lett.* **75**, 4326 (1995).
- [16] K. Kruse, J.-F. Joanny, F. Jülicher, J. Prost, and K. Sekimoto, *Phys. Rev. Lett.* **92**, 078101 (2004).
- [17] M. C. Marchetti, J.-F. Joanny, S. Ramaswamy, T. B. Liverpool, J. Prost, M. Rao, and R. A. Simha, *Rev. Mod. Phys.* **85**, 1143 (2013).
- [18] R. Wittkowski, A. Tiribocchi, J. Stenhammar, R. J. Allen, D. Marenduzzo, and M. E. Cates, *Nat. Commun.* **5**, 4351 (2014).
- [19] T. Vicsek, A. Czirók, E. Ben-Jacob, I. Cohen, and O. Shochet, *Phys. Rev. Lett.* **75**, 1226 (1995).
- [20] M. E. Cates, *Rep. Prog. Phys.* **75**, 042601 (2012).
- [21] P. Romanczuk, M. Bär, W. Ebeling, B. Lindner, and L. Schimansky-Geier, *Eur. Phys. J.: Spec. Top.* **202**, 1 (2012).
- [22] É. Fodor and M. C. Marchetti, *Physica A (Amsterdam)* **504**, 106 (2018).
- [23] M. J. Schnitzer, *Phys. Rev. E* **48**, 2553 (1993).
- [24] Y. Fily and M. C. Marchetti, *Phys. Rev. Lett.* **108**, 235702 (2012).
- [25] J. Elgeti and G. Gompper, *Europhys. Lett.* **85**, 38002 (2009).
- [26] J. Tailleur and M. E. Cates, *Europhys. Lett.* **86**, 60002 (2009).
- [27] P. Galajda, J. Keymer, P. Chaikin, and R. Austin, *J. Bacteriol.* **189**, 8704 (2007).
- [28] R. Di Leonardo, L. Angelani, D. Dell'Arciprete, G. Ruocco, V. Iebba, S. Schippa, M. P. Conte, F. Mecarini, F. De Angelis, and E. Di Fabrizio, *Proc. Natl. Acad. Sci. USA* **107**, 9541 (2010).
- [29] A. Sokolov, M. M. Apodaca, B. A. Grzybowski, and I. S. Aranson, *Proc. Natl. Acad. Sci. USA* **107**, 969 (2010).
- [30] N. Koumakis, C. Maggi, and R. Di Leonardo, *Soft Matter* **10**, 5695 (2014).
- [31] P. Pietzonka, E. Fodor, C. Lohrmann, M. E. Cates, and U. Seifert, *Phys. Rev. X* **9**, 041032 (2019).
- [32] G. Grégoire and H. Chaté, *Phys. Rev. Lett.* **92**, 025702 (2004).
- [33] J. Tailleur and M. E. Cates, *Phys. Rev. Lett.* **100**, 218103 (2008).
- [34] M. E. Cates and J. Tailleur, *Annu. Rev. Condens. Matter Phys.* **6**, 219 (2015).
- [35] É. Fodor, H. Hayakawa, J. Tailleur, and F. van Wijland, *Phys. Rev. E* **98**, 062610 (2018).
- [36] G. Szamel, *Phys. Rev. E* **90**, 012111 (2014).
- [37] C. Maggi, U. Marini Bettolo Marconi, N. Gnan, and R. Di Leonardo, *Sci. Rep.* **5**, 10742 (2015).
- [38] U. Marini Bettolo Marconi and C. Maggi, *Soft Matter* **11**, 8768 (2015).
- [39] G. Szamel, E. Flenner, and L. Berthier, *Phys. Rev. E* **91**, 062304 (2015).
- [40] T. F. F. Farage, P. Krininger, and J. M. Brader, *Phys. Rev. E* **91**, 042310 (2015).
- [41] E. Fodor, C. Nardini, M. E. Cates, J. Tailleur, P. Visco, and F. van Wijland, *Phys. Rev. Lett.* **117**, 038103 (2016).

- [42] R. Wittmann, C. Maggi, A. Sharma, A. Scacchi, J. M. Brader, and U. M. B. Marconi, *J. Stat. Mech.: Theory Exp.* (2017) 113207.
- [43] R. Wittmann, U. M. B. Marconi, C. Maggi, and J. M. Brader, *J. Stat. Mech.* (2017) 113208.
- [44] U. Marini Bettolo Marconi, C. Maggi, and M. Paoluzzi, *J. Chem. Phys.* **147**, 024903 (2017).
- [45] L. Caprini, U. M. B. Marconi, A. Puglisi, and A. Vulpiani, *J. Stat. Mech.* (2019) 053203.
- [46] L. Caprini, U. M. B. Marconi, and A. Puglisi, *Sci. Rep.* **9**, 1386 (2019).
- [47] C. Maggi, M. Paoluzzi, N. Pellicciotta, A. Lepore, L. Angelani, and R. Di Leonardo, *Phys. Rev. Lett.* **113**, 238303 (2014).
- [48] M. Deforet, V. Hakim, H. Yevick, G. Duclos, and P. Silberzan, *Nat. Commun.* **5**, 3747 (2014).
- [49] V. Hakim and P. Silberzan, *Rep. Prog. Phys.* **80**, 076601 (2017).
- [50] L. Berthier and J. Kurchan, *Nat. Phys.* **9**, 310 (2013).
- [51] L. L. Bonilla, *Phys. Rev. E* **100**, 022601 (2019).
- [52] R. F. Fox, *Phys. Rev. A* **33**, 467 (1986).
- [53] R. F. Fox, *Phys. Rev. A* **34**, 4525 (1986).
- [54] P. Jung and P. Hänggi, *Phys. Rev. A* **35**, 4464 (1987).
- [55] L. Cao, D.-J. Wu, and X.-L. Luo, *Phys. Rev. A* **47**, 57 (1993).
- [56] C. R. Doering, P. S. Hagan, and C. D. Levermore, *Phys. Rev. Lett.* **59**, 2129 (1987).
- [57] C. Van den Broeck and P. Hänggi, *Phys. Rev. A* **30**, 2730 (1984).
- [58] A. P. Solon, Y. Fily, A. Baskaran, M. E. Cates, Y. Kafri, M. Kardar, and J. Tailleur, *Nat. Phys.* **11**, 1745 (2015).
- [59] I. Fredholm, *Acta Math.* **27**, 365 (1903).
- [60] F. Bouchet, K. Gawedzki, and C. Nardini, *J. Stat. Phys.* **163**, 1157 (2016).
- [61] U. M. B. Marconi, N. Gnan, M. Paoluzzi, C. Maggi, and R. Di Leonardo, *Sci. Rep.* **6**, 23297 (2016).
- [62] I. Theurkauff, C. Cottin-Bizonne, J. Palacci, C. Ybert, and L. Bocquet, *Phys. Rev. Lett.* **108**, 268303 (2012).
- [63] J. Palacci, S. Sacanna, A. P. Steinberg, D. J. Pine, and P. M. Chaikin, *Science* **339**, 936 (2013).
- [64] I. Buttinoni, J. Bialké, F. Kümmel, H. Löwen, C. Bechinger, and T. Speck, *Phys. Rev. Lett.* **110**, 238301 (2013).
- [65] C.-W. Io, T.-Y. Chen, J.-W. Yeh, and S.-C. Cai, *Phys. Rev. E* **96**, 062601 (2017).
- [66] D. Geyer, D. Martin, J. Tailleur, and D. Bartolo, *Phys. Rev. X* **9**, 031043 (2019).
- [67] *Course of Theoretical Physics (3rd ed.)*, edited by L. Landau and E. Lifshitz (Pergamon, Oxford, 1980), pp. 79–110.
- [68] N. G. Van Kampen, *Stochastic Processes in Physics and Chemistry* (Elsevier, Amsterdam, 1992), Vol. 1.
- [69] E. Woillez, Y. Kafri, and V. Lecomte, *J. Stat. Mech.* (2020) 063204.
- [70] D. Martin and T. Arnoulx de Pirey, [arXiv:2009.13476](https://arxiv.org/abs/2009.13476).
- [71] M. Serone, G. Spada, and G. Villadoro, *J. High Energy Phys.* **05** (2017) 056.
- [72] P. Jung and P. Hänggi, *J. Opt. Soc. A* **5**, 979 (1988).
- [73] R. F. Fox, *Phys. Rev. A* **37**, 911 (1988).
- [74] A. J. Bray and A. J. McKane, *Phys. Rev. Lett.* **62**, 493 (1989).
- [75] A. J. Bray, A. J. McKane, and T. J. Newman, *Phys. Rev. A* **41**, 657 (1990).
- [76] P. Hänggi and P. Jung, *Adv. Chem. Phys.* **89**, 239 (1995).
- [77] S. Faetti, L. Fronzoni, P. Grigolini, and R. Mannella, *J. Stat. Phys.* **52**, 951 (1988).
- [78] M. Rein and T. Speck, *Eur. Phys. J. E* **39**, 84 (2016).
- [79] M. E. Cates and J. Tailleur, *Europhys. Lett.* **101**, 20010 (2013).
- [80] N. Van Kampen, *IBM J. Res. Dev.* **32**, 107 (1988).
- [81] N. Van Kampen, *J. Phys. Chem. Solids* **49**, 673 (1988).
- [82] E. Bringuer and A. Bourdon, *J. Non-Equilib. Thermodyn.* **32**, 221 (2007).
- [83] A. W. C. Lau and T. C. Lubensky, *Phys. Rev. E* **76**, 011123 (2007).
- [84] M. Yang and M. Ripoll, *Phys. Rev. E* **87**, 062110 (2013).
- [85] S. H. Lim and J. Wehr, *J. Stat. Phys.* **174**, 656 (2019).
- [86] J. Stenhammar, R. Wittkowski, D. Marenduzzo, and M. E. Cates, *Sci. Adv.* **2**, e1501850 (2016).
- [87] G. Liu, A. Patch, F. Bahar, D. Yllanes, R. D. Welch, M. C. Marchetti, S. Thutupalli, and J. W. Shaevitz, *Phys. Rev. Lett.* **122**, 248102 (2019).
- [88] D. Chowdhury, L. Santen, and A. Schadschneider, *Phys. Rep.* **329**, 199 (2000).
- [89] D. Helbing, *Rev. Mod. Phys.* **73**, 1067 (2001).
- [90] T. Nagatani, *Rep. Prog. Phys.* **65**, 1331 (2002).
- [91] G. S. Redner, M. F. Hagan, and A. Baskaran, *Phys. Rev. Lett.* **110**, 055701 (2013).
- [92] J. Stenhammar, D. Marenduzzo, R. J. Allen, and M. E. Cates, *Soft Matter* **10**, 1489 (2014).
- [93] A. Wysocki, R. G. Winkler, and G. Gompper, *Europhys. Lett.* **105**, 48004 (2014).
- [94] A. Solon, M. Cates, and J. Tailleur, *Eur. Phys. J.: Spec. Top.* **224**, 1231 (2015).
- [95] A. Solon, J. Stenhammar, M. E. Cates, Y. Kafri, and J. Tailleur, *New J. Phys.* **20**, 075001 (2018).
- [96] E. Tjhung, C. Nardini, and M. E. Cates, *Phys. Rev. X* **8**, 031080 (2018).
- [97] C. B. Caporusso, P. Digregorio, D. Levis, L. F. Cugliandolo, and G. Gonnella, *Phys. Rev. Lett.* **125**, 178004 (2020).
- [98] X.-q. Shi, G. Fausti, H. Chaté, C. Nardini, and A. Solon, *Phys. Rev. Lett.* **125**, 168001 (2020).
- [99] C. Maggi, M. Paoluzzi, A. Crisanti, E. Zaccarelli, and N. Gnan, [arXiv:2007.12660](https://arxiv.org/abs/2007.12660).
- [100] D. Levis and L. Berthier, *Phys. Rev. E* **89**, 062301 (2014).
- [101] J. U. Klamser, S. C. Kapfer, and W. Krauth, *Nat. Commun.* **9**, 5045 (2018).
- [102] V. Dossetti and F. J. Sevilla, *Phys. Rev. Lett.* **115**, 058301 (2015).
- [103] Y. Fily, Y. Kafri, A. P. Solon, J. Tailleur, and A. Turner, *J. Phys. A: Math. Theor.* **51**, 044003 (2017).
- [104] S. C. Takatori, W. Yan, and J. F. Brady, *Phys. Rev. Lett.* **113**, 028103 (2014).
- [105] S. Paliwal, J. Rodenburg, R. van Roij, and M. Dijkstra, *New J. Phys.* **20**, 015003 (2018).
- [106] T. Arnoulx de Pirey, G. Lozano, and F. van Wijland, *Phys. Rev. Lett.* **123**, 260602 (2019).
- [107] J. Bickmann and R. Wittkowski, *J. Phys.: Condens. Matter* **32**, 214001 (2020).

- [108] J. H. Irving and J. G. Kirkwood, *J. Chem. Phys.* **18**, 817 (1950).
- [109] Y. Pomeau, Surface tension: From fundamental principles to applications in liquids and in solids, Lecture Notes of the Fifth Warsaw School of Statistical Physics (unpublished).
- [110] J. Yvon, *Colloque de Thermodynamique, Bruxelles, Janvier 1948: Symposium on Thermodynamics* (Imprimeurs, Paris, 1949), pp. 9–15.
- [111] A. P. Solon, J. Stenhammar, R. Wittkowski, M. Kardar, Y. Kafri, M. E. Cates, and J. Tailleur, *Phys. Rev. Lett.* **114**, 198301 (2015).
- [112] M. E. Fisher, *J. Chem. Phys.* **42**, 3852 (1965).
- [113] J. Bialké, H. Löwen, and T. Speck, *Europhys. Lett.* **103**, 30008 (2013).
- [114] X. Yang, M. L. Manning, and M. C. Marchetti, *Soft Matter* **10**, 6477 (2014).
- [115] J. M. Epstein, K. Klymko, and K. K. Mandadapu, *J. Chem. Phys.* **150**, 164111 (2019).
- [116] T. Bäuerle, A. Fischer, T. Speck, and C. Bechinger, *Nat. Commun.* **9**, 3232 (2018).
- [117] D. S. Dean, *J. Phys. A: Math. Gen.* **29**, L613 (1996).
- [118] A. P. Solon, J. Stenhammar, M. E. Cates, Y. Kafri, and J. Tailleur, *Phys. Rev. E* **97**, 020602(R) (2018).
- [119] U. Seifert, *Rep. Prog. Phys.* **75**, 126001 (2012).
- [120] D. J. Evans, E. G. D. Cohen, and G. P. Morriss, *Phys. Rev. Lett.* **71**, 2401 (1993).
- [121] G. Gallavotti and E. G. D. Cohen, *Phys. Rev. Lett.* **74**, 2694 (1995).
- [122] J. Kurchan, *J. Phys. A: Math. Gen.* **31**, 3719 (1998).
- [123] J. L. Lebowitz and H. Spohn, *J. Stat. Phys.* **95**, 333 (1999).
- [124] C. Maes, *J. Stat. Phys.* **95**, 367 (1999).
- [125] T. Speck, *Europhys. Lett.* **114**, 30006 (2016).
- [126] U. M. B. Marconi, A. Puglisi, and C. Maggi, *Sci. Rep.* **7**, 46496 (2017).
- [127] P. Pietzonka and U. Seifert, *J. Phys. A: Math. Theor.* **51**, 01LT01 (2017).
- [128] D. Mandal, K. Klymko, and M. R. DeWeese, *Phys. Rev. Lett.* **119**, 258001 (2017).
- [129] S. Shankar and M. C. Marchetti, *Phys. Rev. E* **98**, 020604(R) (2018).
- [130] S. Chaki and R. Chakrabarti, *Physica A (Amsterdam)* **511**, 302 (2018).
- [131] L. Dabelow, S. Bo, and R. Eichhorn, *Phys. Rev. X* **9**, 021009 (2019).
- [132] L. Caprini, U. M. B. Marconi, A. Puglisi, and A. Vulpiani, *Phys. Rev. Lett.* **121**, 139801 (2018).
- [133] S. Chaki and R. Chakrabarti, *Physica A (Amsterdam)* **530**, 121574 (2019).
- [134] T. GrandPre, K. Klymko, K. K. Mandadapu, and D. T. Limmer, *Phys. Rev. E* **103**, 012613 (2021).
- [135] E. Flenner and G. Szamel, *Phys. Rev. E* **102**, 022607 (2020).
- [136] A. Ajdari and J. Prost, *Comptes rendus de l'Académie des sciences. Série 2, Mécanique, Physique, Chimie, Sciences de l'univers, Sciences de la Terre* **315**, 1635 (1992).
- [137] M. O. Magnasco, *Phys. Rev. Lett.* **71**, 1477 (1993).
- [138] L. Angelani, R. Di Leonardo, and G. Ruocco, *Phys. Rev. Lett.* **102**, 048104 (2009).
- [139] N. Kumar, R. K. Gupta, H. Soni, S. Ramaswamy, and A. K. Sood, *Phys. Rev. E* **99**, 032605 (2019).
- [140] M. B. Wan, C. J. Olson Reichhardt, Z. Nussinov, and C. Reichhardt, *Phys. Rev. Lett.* **101**, 018102 (2008).
- [141] L. Angelani, A. Costanzo, and R. Di Leonardo, *Europhys. Lett.* **96**, 68002 (2011).
- [142] C. O. Reichhardt and C. Reichhardt, *Annu. Rev. Condens. Matter Phys.* **8**, 51 (2017).
- [143] L. Onsager and S. Machlup, *Phys. Rev.* **91**, 1505 (1953).
- [144] T. Ekeh, M. E. Cates, and É. Fodor, *Phys. Rev. E* **102**, 010101(R) (2020).
- [145] T. Speck, J. Bialké, A. M. Menzel, and H. Löwen, *Phys. Rev. Lett.* **112**, 218304 (2014).
- [146] F. Caballero, C. Nardini, F. van Wijland, and M. E. Cates, *Phys. Rev. Lett.* **121**, 020601 (2018).
- [147] C. Nardini, E. Fodor, E. Tjhung, F. van Wijland, J. Tailleur, and M. E. Cates, *Phys. Rev. X* **7**, 021007 (2017).
- [148] F. Caballero, C. Nardini, and M. E. Cates, *J. Stat. Mech.* (2018) 123208.
- [149] D. Andrieux, P. Gaspard, S. Ciliberto, N. Garnier, S. Joubaud, and A. Petrosyan, *Phys. Rev. Lett.* **98**, 150601 (2007).
- [150] É. Roldán, J. Barral, P. Martin, J. M. Parrondo, and F. Jülicher, [arXiv:1803.04743](https://arxiv.org/abs/1803.04743).
- [151] M. Baiesi and C. Maes, *New J. Phys.* **15**, 013004 (2013).
- [152] G. Szamel, *Europhys. Lett.* **117**, 50010 (2017).
- [153] L. Caprini, U. M. B. Marconi, and A. Vulpiani, *J. Stat. Mech.* (2018) 033203.
- [154] S. Dal Cengio, D. Levis, and I. Pagonabarraga, *Phys. Rev. Lett.* **123**, 238003 (2019).
- [155] S. D. Cengio, D. Levis, and I. Pagonabarraga, [arXiv:2007.07322](https://arxiv.org/abs/2007.07322).
- [156] C. Maes, *Front. Phys.* **8**, 229 (2020).
- [157] L. F. Cugliandolo, *J. Phys. A: Math. Gen.* **44**, 483001 (2011).
- [158] G. Agarwal, *Z. Phys.* **252**, 25 (1972).
- [159] J. Prost, J.-F. Joanny, and J. M. R. Parrondo, *Phys. Rev. Lett.* **103**, 090601 (2009).
- [160] F. Kümmel, B. ten Hagen, R. Wittkowski, I. Buttinoni, R. Eichhorn, G. Volpe, H. Löwen, and C. Bechinger, *Phys. Rev. Lett.* **110**, 198302 (2013).
- [161] J. Palacci, S. Sacanna, S.-H. Kim, G.-R. Yi, D. Pine, and P. Chaikin, *Philos. Trans. R. Soc. A* **372**, 20130372 (2014).
- [162] J. M. Walter, D. Greenfield, C. Bustamante, and J. Liphardt, *Proc. Natl. Acad. Sci. USA* **104**, 2408 (2007).
- [163] G. Vizsnyiczai, G. Frangipane, C. Maggi, F. Saglimbeni, S. Bianchi, and R. Di Leonardo, *Nat. Commun.* **8**, 15974 (2017).
- [164] G. Frangipane, D. Dell'Arciprete, S. Petracchini, C. Maggi, F. Saglimbeni, S. Bianchi, G. Vizsnyiczai, M. L. Bernardini, and R. Di Leonardo, *Elife* **7**, e36608 (2018).
- [165] J. Arlt, V. A. Martinez, A. Dawson, T. Pilizota, and W. C. K. Poon, *Nat. Commun.* **9**, 768 (2018).
- [166] J. Arlt, V. A. Martinez, A. Dawson, T. Pilizota, and W. C. K. Poon, *Nat. Commun.* **10**, 2321 (2019).
- [167] M. Baiesi, U. Basu, and C. Maes, *Eur. Phys. J. B* **87**, 277 (2014).
- [168] K. Kawasaki, *Physica A (Amsterdam)* **208**, 35 (1994).
- [169] A. Campa, T. Dauxois, and S. Ruffo, *Phys. Rep.* **480**, 57 (2009).
- [170] J. Stenhammar, C. Nardini, R. W. Nash, D. Marenduzzo, and A. Morozov, *Phys. Rev. Lett.* **119**, 028005 (2017).
- [171] M. Doi and S. F. Edwards, *The Theory of Polymer Dynamics* (Oxford University Press, Oxford, 1988), Vol. 73.

- [172] D. A. Dawson and J. Gärtner, *Stochastics: Int. J. Probab. Stochastic Proc.* **20**, 247 (1987).
- [173] T. Nakamura and A. Yoshimori, *J. Phys. A: Math. Theor.* **42**, 065001 (2009).
- [174] S. P. Das and G. F. Mazenko, *Phys. Rev. A* **34**, 2265 (1986).
- [175] R. Schmitz, J. W. Dufty, and P. De, *Phys. Rev. Lett.* **71**, 2066 (1993).
- [176] A. J. Archer, *J. Phys.: Condens. Matter* **18**, 5617 (2006).
- [177] A. J. Archer, *J. Chem. Phys.* **130**, 014509 (2009).
- [178] S. P. Das and A. Yoshimori, *Phys. Rev. E* **88**, 043008 (2013).
- [179] V. Démery, *Phys. Rev. E* **91**, 062301 (2015).
- [180] K. Klymko, D. Mandal, and K. K. Mandadapu, *J. Chem. Phys.* **147**, 194109 (2017).
- [181] F. Cagnetta, F. Corberi, G. Gonnella, and A. Suma, *Phys. Rev. Lett.* **119**, 158002 (2017).
- [182] L. Tociu, E. Fodor, T. Nemoto, and S. Vaikuntanathan, *Phys. Rev. X* **9**, 041026 (2019).
- [183] T. Nemoto, E. Fodor, M. E. Cates, R. L. Jack, and J. Tailleur, *Phys. Rev. E* **99**, 022605 (2019).
- [184] É. Fodor, T. Nemoto, and S. Vaikuntanathan, *New J. Phys.* **22**, 013052 (2020).
- [185] U. G. Haussmann and E. Pardoux, *Ann. Probab.* **14**, 1188 (1986).
- [186] J. R. Norris, *Markov Chains* (Cambridge University Press, Cambridge, 1998), Vol. 2.
- [187] G. A. Pavliotis, *Stochastic Processes and Applications* (Springer, Berlin, 2016).
- [188] G. Falasco and M. Baiesi, *Europhys. Lett.* **113**, 20005 (2016).
- [189] G. Falasco and M. Baiesi, *New J. Phys.* **18**, 043039 (2016).